CORROSION CHARACTERIZATION OF OPTIMIZED ZrO_2-SiO_2 MIXED NANOTUBES COATED ON ALUMINIUM ALLOY AA3003

SHALINI DEVI RAMAIYA

FACULTY OF ENGINEERING
UNIVERSITY OF MALAYA
KUALA LUMPUR

2018

CORROSION CHARACTERIZATION OF OPTIMIZED ZrO_2-SiO_2 MIXED NANOTUBES COATED ON ALUMINIUM ALLOY AA3003

SHALINI DEVI RAMAIYA

RESEARCH REPORT SUBMITTED IN PARTIAL FULFILMENTOF THE REQUIREMENTSFOR THE DEGREE OF MASTER OF MATERIALS ENGINEERING

FACULTY OF ENGINEERING
UNIVERSITY OF MALAYA
KUALA LUMPUR

2018

UNIVERSITY OF MALAYA

ORIGINAL LITERARY WORK DECLARATION

Name of Candidate: **Shalini Devi Ramaiya**

Matric No: **KQJ170010**

Name of Degree: **Master of Materials Engineering**

Title of Project Paper/Research Report/Dissertation/Thesis ("this Work"):

"Corrosion characterization of optimized ZrO_2-SiO_2 mixed nanotubes coated on aluminium alloy AA3003"

Field of Study: Corrosion Engineering

I do solemnly and sincerely declare that:

(1) I am the sole author/writer of this Work;
(2) This Work is original;
(3) Any use of any work in which copyright exists was done by way of fair dealing and for permitted purposes and any excerpt or extract from, or reference to or reproduction of any copyright work has been disclosed expressly and sufficiently and the title of the Work and its authorship have been acknowledged in this Work;
(4) I do not have any actual knowledge nor do I ought reasonably to know that the making of this work constitutes an infringement of any copyright work;
(5) I hereby assign all and every rights in the copyright to this Work to the University ofMalaya ("UM"), who henceforth shall be owner of the copyright in this Work and that any reproduction or use in any form or by any means whatsoever is prohibited without the written consent of UM having been first had and obtained;
(6) I am fully aware that if in the course of making this Work I have infringed any copyright whether intentionally or otherwise, I may be subject to legal action or any other action as may be determined by UM.

Candidate's Signature Date:

Subscribed and solemnly declared before,

Witness's Signature Date:

Name:

Designation:

ABSTRACT

Aluminium (Al) alloys are most important materials for the applications in cutting tools, engine block, as well as marine and aerospace components. In the present study, surface modification of Al alloy series 3, which known as aluminium-manganese alloy specifically AA3003, was carried out by deposition of a Zr-Si thin film as a coating layer using physical vapor deposition magnetron sputtering (PVDMS) method. Well-adhered ZrO_2-SiO_2 mixed nanotubular arrays were successfully grown on AA3003 by anodization method, then by heat treatment using temperature in the range of 500–700 °C for 1.5 h under atmospheric condition. The surface wettability, microhardness and corrosion behavior were studied. From the microstructural analysis, the average length and diameter of the optimized nanotubular arrays ranged from 0.6 μm and 0.5 μm. For the 600 °C annealed sample with the strongest adhesion, the scratch length, failure point and adhesion strength were 985.94 μm, 812.88μm and 2700.28 mN, respectively. Besides, the annealed coating showed the highest wettability (lowest contact angle value). Potentiodynamic polarization results indicated that the corrosion rate decreased after deposition of Zr-Si thin film, anodization and thermal treatment compared to the bare substrate.

ABSTRAK

Aluminium merupakan bahan yang paling penting untuk aplikasi dalam alat pemotong, blok enjin serta komponen marin dan aeroangkasa. Dalam kajian ini, pengubahsuaian permukaan untuk aluminium aloi siri 3 yang juga dikenali sebagai aloi aluminium mangan khususnya AA3003, telah dilakukan oleh pemendapan filem nipis Zr-Si sebagai lapisan salutan dengan mengunakan kaedah pemendapan wap fizikan mangnetron spettering (PVDMS). Susunan nanotubular campuran ZrO_2-SiO_2 yang telah dipatenkan berjaya ditanam pada AA3003 dengan kaedah anodisasi, diikuti dengan rawatan haba dalam julat suhu 500-700 ° C selama 1.5 jam di bawah keadaan atmosfera. Kebolehbahan permukaan, mikrohard dan tingkah laku kakisan telah dipelajari. Dari sudut pandangan microstructural, panjang purata dan garis pusat susunan nanotubular yang dioptimumkan adalah dari 0.6 μm dan 0.5 μm. Untuk sampel anneal 600 ° C dengan lekatan terkuat, panjang goresan, titik kegagalan dan kekuatan lekatan adalah 985.94 μm, 812.88 μm dan 2700.28 mN. Selain itu, salutan anil menunjukkan kebolehdayaan tertinggi (nilai sudut sentuhan terendah). Hasil polarisasi potentiodinamik menunjukkan bahawa kadar karat menurun selepas pemendapan filem tipis Zr-Si, anodisasi dan rawatan haba berbanding dengan substrat kosong.

ACKNOWLEDGEMENTS

At the outset, I thank to god almighty for making this project as a successful one.

I would like to take this opportunity to express my gratitude and deep regards to my supervisor, Dr. Nazatul Liana Binti Sukiman for her excellent supervision and constant support which helps much in completing my research project with great success and given time frame. I shall forever carry the knowledge, guidance and support provided by her throughout my journey in pursuit my life. I truly appreciate and value everything that I learned here. Her lead throughout the experimental and thesis works have contributed to the success of this project.

I would like to express my special thanks to Dr. Masoud sarraf for his endless guidance and motivation from the very beginning of the project until the very end. Special thanks goes to all the staffs from faculty of engineering, who gave permission to use all required machines and needed materials to complete my experiment without any obstacles.

I would like to extend my thankfulness to the most precious person in my life, my parents, for all their moral support, financial support and also to my siblings and friends for their never ending encouragement to complete my project work.

Last but not least, my deepest gratitude goes to everyone whom directly or indirectly helped me to complete my experiment and thesis as well. Thank you very much.

TABLE OF CONTENTS

LIST OF FIGURES

LIST OF TABLES

LIST OF SYMBOLS AND ABBREVIATIONS

PVD	:	Physical vapour deposition
NTs	:	Nanotubes
Al	:	Aluminium
ZrO_2	:	Zirconia/ zirconium dioxide
SiO_2	:	Silica/ Solicon dioxide
Icorr	:	Corrosion current density
Ecorr	:	Corrosion potential
Zr	:	Zirconium
Si	:	Silicon
FESEM	:	Field Emission Scanning Electron Microscope
XRD	:	X-Ray Diffraction
EDXS	:	Energy Dispersive Spectrometry
PE	:	Effectiveness of corrosion protection
HV	:	Vickers hardness value
CVD	:	Chemical vapour deposition
PDP	:	Potentiodynamic polarization
Al_2O_3	:	Alumina/ aluminium oxide
AC	:	Alternate current
DC	:	Direct current
Icorr	:	Corrosion current density
Ecorr	:	Corrosion Potential

CHAPTER 1 : INTRODUCTION

1.1 Background study

Aluminium casting alloys are extensively applied in many sectors such as automobile parts, cutting tools, structures, aerospace parts and so on. Aluminium alloys are well known for their excellent properties as compared to other elements. Automotive industry widely uses aluminium alloys due to their light weight, which makes the vehicle weight much lighter compared to other metals. Thus, the lighter the weight of the vehicle leads to the lower the fuel consumption of a vehicle (Doty *et al.*, 2003). It is reported that using aluminium radiator, 37% of weight saving can be achieved and save cost as well (Leeuw, 1999).

The current automotive industry uses aluminium alloys series 3 (for example AA3102, AA3003 and AA3103) to manufacture the engine parts due to its high strength, light weight and extrudability. Aluminium alloys were first used for automotive heat exchanger components, which then progressively evolved into applications including both engine cooling and air conditioning systems. The system wrapped up with condenser, the evaporator and refrigerant routing lines or fluid carrying lines (Ole Daaland *et al*., 1999).

However, the aluminium made engine parts basically subjected to some conditions during operation such as mechanical loading, vibration, stone impingement, and road chemicals (Ole Daaland *et al*., 1999). The road chemicals here denote the salt water environment. The bare aluminium alloy (AA3003) substrate surface however can be easily attacked when it is exposed to the corrosive environment, which causes severe pitting corrosion and reduces the life span of the parts. This causes catastrophic failure of the automotive components over the period of time.

Hence, the best method to improve the resistivity towards corrosion and overcome the major drawback of AA3003, modification of surface is necessary. There

are several types of surface modification techniques used to modify the surface such as PVD process, CVD process, electroless coatings, nitriding, thermal spraying, surface welding, ion implantation, anodizing, and thermal hardening. Therefore, with the aid of PVD method a thin film of Zr and Si was deposited on the substrate. By anodizing technique, ZrO_2-SiO_2 nanotubes were obtained, which increased wear resistance, formed non-conductive barrier against release of the ions, improved wettability and corrosion resistance, and provided passages for facilitated penetration of the electrolyte within the oxide later.

Zirconium dioxide or known as zirconia (ZrO_2) is famously known for its excellent mechanical properties such as high resistance to corrosion, low thermal conductivity and high melting point. It is also compatible for corrosion resistant coating, for example chemical durability and good thermal shock characteristics. Besides that, oxides itself has high mechanical toughness which makes them to use in various of applications (Ganapathy, V *et al.*, 2018).

Silicon dioxide or silica (SiO_2) has outstanding properties such as high hardness with excellent flexibility, thermal stability, corrosion resistance and good adhesion (Pathal,S.S *et al.*, 2009). It can also allow strain relaxation without mechanical fracture during processing period (Park, M.H *et al.*, 2009).

Heat treatment was conducted to enhance the mechanical properties and form highly crystalline ZrO_2-SiO_2 (anatase and rutile) on the surface (M. Sarraf *et al.*, 2015). Apart from that, the nanotubes ZrO_2-SiO_2 shall be identified from characterization method using field emission scanning electron microscopy (FESEM).

1.2 Problem statement

Even though the Al casting alloys are widely used in industry, and it is commonly known for its unique properties such as light weight, well castability, however the issues based on corrosion activity has become a major drawback. Moreover, the behavior and characteristics of aluminium have been studied extensively in recent years, however there is no study on the surface modification of AA3003 by using PVD method. Apart from that, there are many challenges on the corrosion behavior of the modified surface of AA3003 with ZrO_2-SiO_2 NT arrays as well.

1.3 Research Objectives

This study is aim to fabricate and develop highly ordered optimized ZrO_2-SiO_2 NT arrays by PVD of zirconium and silicon layer on Al alloy (AA3003). Besides that, it is also aim to study the corrosion behavior of optimized ZrO_2-SiO_2 nanotubes on modified aluminium alloy series 3 (aluminium-manganese alloy, AA3003).

1.4 Research Scope

The present study aims to fabricate ZrO_2-SiO_2 nanotubes on aluminium alloy (AA3003) to obtain a modified surface which improves its mechanical and corrosion properties for engine application. The development such excellent modified surface aluminium alloy (AA3003) requires several experimental procedures such as it begins with deposition of thin film by PVD magnetron sputtering, anodization and heat treatment. Besides that, the modified surface of aluminium alloy (AA3003) which fabricated with optimized ZrO_2-SiO_2 nanotubes also characterized in the aspects corrosion behavior. The deposited thin film was determined using field emission scanning microscopy (FESEM) to determine the morphological properties. Apart from that, X-ray diffractometry (XRD) and energy dispersive spectroscopy (EDS) were used for phase and chemical analysis, respectively. Besides, the behavior of the thin film was

determined by performing adhesion, microhardness, wear, and wettability as well as corrosion tests by PDP.

1.5 Thesis outline

Chapter 1 consisted of a brief introduction of the research topic and the limitation that faced by the existing methods. Thus, in order to improve the highlighted limitation which is known to be problem statement, aim and objectives were outlined. Scope of study was plotted. In chapter 2, a thorough background study was conducted based on the research title which is ZrO_2-SiO_2 thin film on the aluminium alloy (AA3003) substrate. This chapter also includes the process overview, advantages, techniques and application that used throughout fabricating the ZrO_2-SiO_2 nanotubes on aluminium alloy (AA3003) substrate. Chapter 3 explains about the methodology used in order to prepare ZrO_2-SiO_2 nanotubes on aluminium alloy (AA3003) substrate as well as the methods that used to analyze the characterization of the deposited thin film such as morphological, mechanical, corrosion, chemical and tribology. In chapter 4, the analysis of the results were discussed which leads to draw a conclusion and propose some recommendation in chapter 5. The flow of the project is plotted in Figure 1.1.

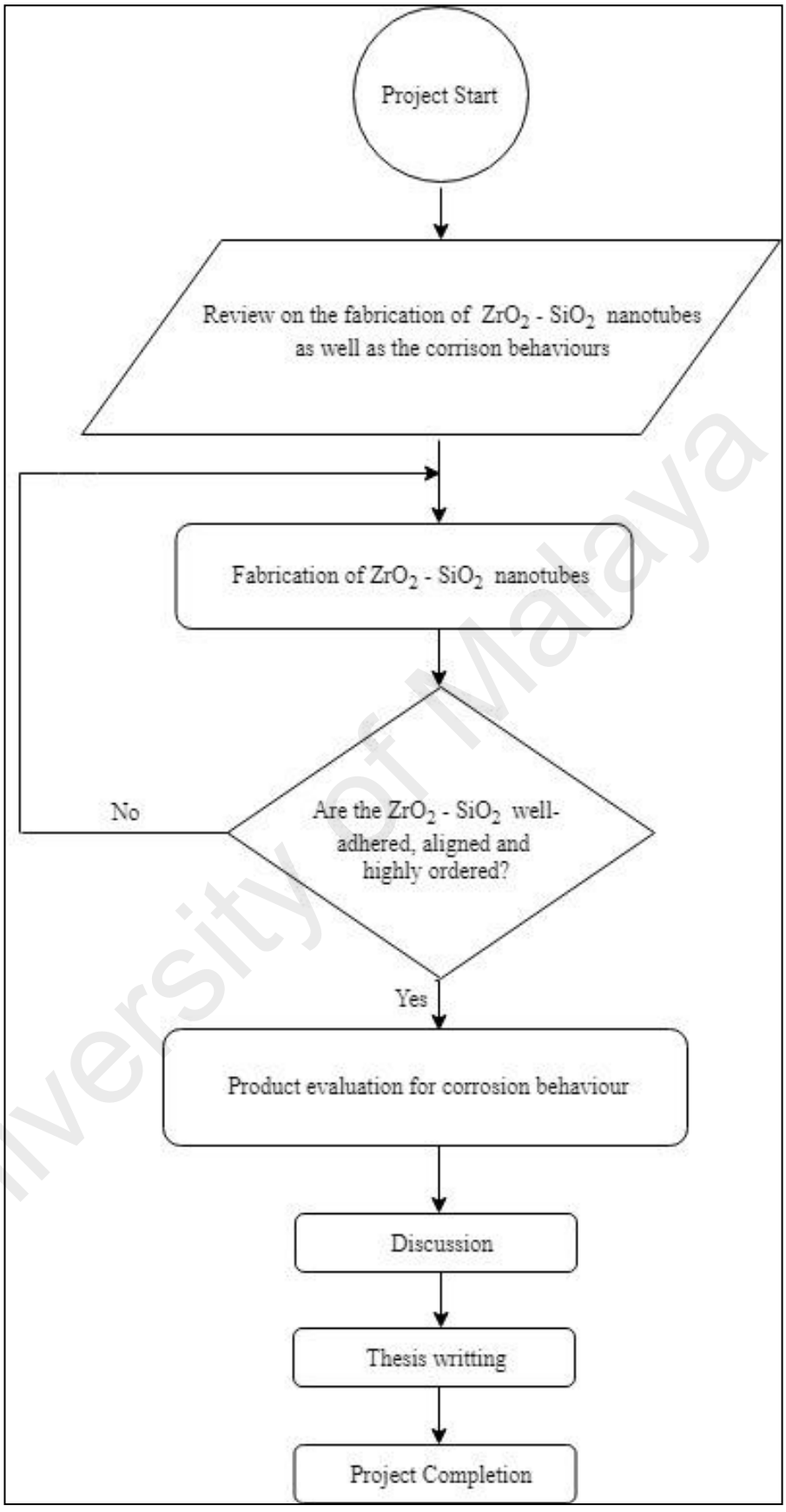

Figure 1: Flow chart of the project

CHAPTER 2: LITERATURE REVIEW

2.1 Aluminium

Aluminium is basically considered as the most abundant metal in the world and it comprises 8% of the earth crust, which is the third most common element. Besides steel, aluminium is the mostly used element today. Aluminium is a widely used metal in industry due to its special characteristics and behavior. In general, aluminium has its own unique characteristics. Aluminium has the ability to combine with other elements and form most of the gems such as sapphine, ruby, and emerald. Aluminium ores most likely to be found in tropical climate and more rainfall favored places. The common ore of aluminium that exist is Bauxite (aluminium oxide). The name emerged after the place called Les Baux, in France in 1821.

Approximately 30Mt per annum (32Mt of primary aluminium and +30% of secondary aluminium (recycled scraps) is produced globally in 2006 (robeul *et al.*).In year 2005, global product aluminium was 32 million tons, whereas in 2015, global production was about 58 million tons. According to European Aluminium Association, it has been estimated that the weight of the car still can be reduced by 36% by increasing the use of aluminium. Hence, aluminium plays a vital role in automotive industry. Initially, engine blocks are manufactured from cast iron which then substitute by aluminium alloy A319 and AA356. Aluminium alloy is use to make engine blocks due to its light weight and wear resistance (W.Martienssen,*et al*., 2004).

Aluminium can be categorized as pure, unalloyed or refined which is based on the purification level. Aluminium has its very own unique properties such as it is considered as a light weight element. In comparison, the lightness of aluminium is 30% that of iron, and 35% that of copper. Naturally it has the highest corrosion resistance to

corrosion which can be further enhance through the formation of aluminium alloy. Moreover, the corrosion occurs atmospherically is almost insignificant. Besides that, it demonstrates excellent strength to weight ratio and high reflectivity of light and heat which is up to 80%. Aluminium looks silvery in appearance and it has excellent workability (R.V.Singh, 2011).

Apart from that, aluminium has high electrical and thermal conductivity as well as high elasticity which make it appropriate for shock load condition. The toughness at low temperature is a special asset of aluminium whereby steel is reasonably poorer. Besides that, it has very excellent castability and good weldability that gives the ability to accept almost all finishing processes. In general, aluminium also has high corrosion resistance in majority of service condition and there is no color salts are produced to stain adjoining surfaces. Aluminium also has the tendency to improve its physical properties under cryogenic conditions as well as no toxic reaction encountered by the element itself. The aluminium alloys gives the availability of a wide range of strength, elongation and surface hardness depending on the classification of series (R.V.Singh, 2011).

Aluminium also has an excellent reflector of radiant energy of all wavelength (UV to IR), electromagnetic waves and heat waves. It also has the ability to accept all joining processes including adhesion. Lastly, aluminium is absolutely profitable and easy to recycle (R.V.Singh, 2011).

2.1.1 General properties of aluminium

Aluminium known as a very strong base which make it a fairly reactive element as per shown in electrochemical series. It has low standard potential of -1.66V. Hence, the element cannot be obtained from aqueous solution by electrolysis process. Besides that, carbothermic reaction is also not a proper method to use in order to attain

aluminium element. Therefore, this element is non-flammable and likely chippings and turning does not ignite. However, exceptionally fine particles of aluminium can undergo spontaneous combustion which may leads to explosion.

Table 2.1: Properties of aluminium (R.V.Singh, 2001)

Properties	**Value**
Density	2.71 g/cm3
Melting Point	658 °C
Boiling Point	2480 °C
Thermal expansion	23.5/ K 10^6
Modulus of elasticity	$7.2*10^4$ N/mm^2
Thermal conductivity	2.2 W/cm.K
Electrical conductivity	34-36 m/ohm.mm^2
Atomic number	13
Poison Ratio	0.34
Crystal Lattice	Face centered cubic, FCC

2.1.2 Applications of Aluminium

Aluminium is widely used in many sectors to its special and unique properties such as lightness, corrosion resistance, strength, reflectivity, look, workability, electrical conductivity, thermal conductivity, elasticity, toughness at low temperature and barrier properties. The sectors that mainly use aluminium are transportation, electrical industry, building and architecture, packaging, chemical and food, machine parts, household, space and cast-antiques.

According to European Aluminium Association, it has been estimated that the weight of the car still can be reduced by 36% by increasing the use of aluminium. Hence, aluminium plays a vital role in automotive industry. Initially, engine blocks are manufactured from cast iron which then substitute by aluminium alloy A319 and AA356. Aluminium alloy is use to make engine blocks due to its light weight and wear resistance. The light weight property of aluminium helps to reduce the fuel consumption in automobile industry.

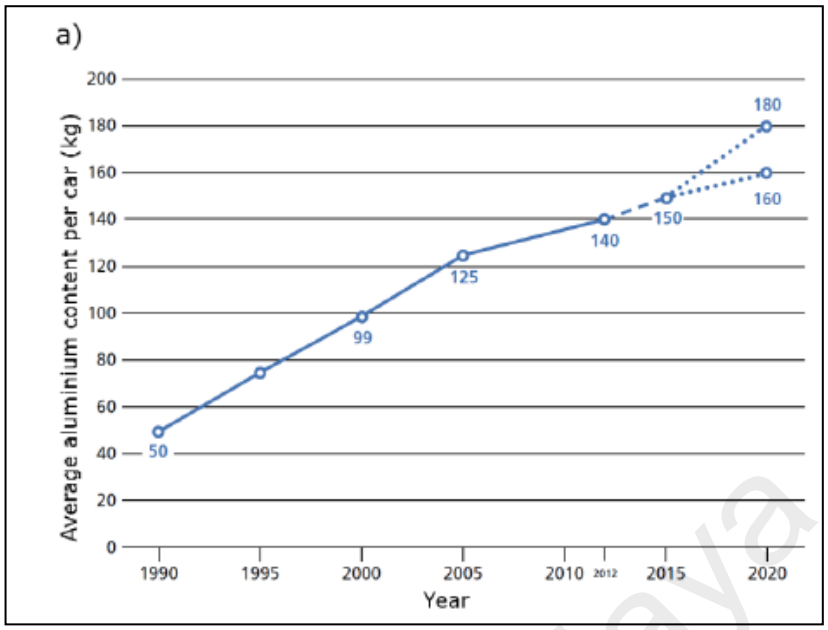

Figure 2.1: Evolution of average Al content per car produced in Europe (W.Martienssen,*et al*., 2004).

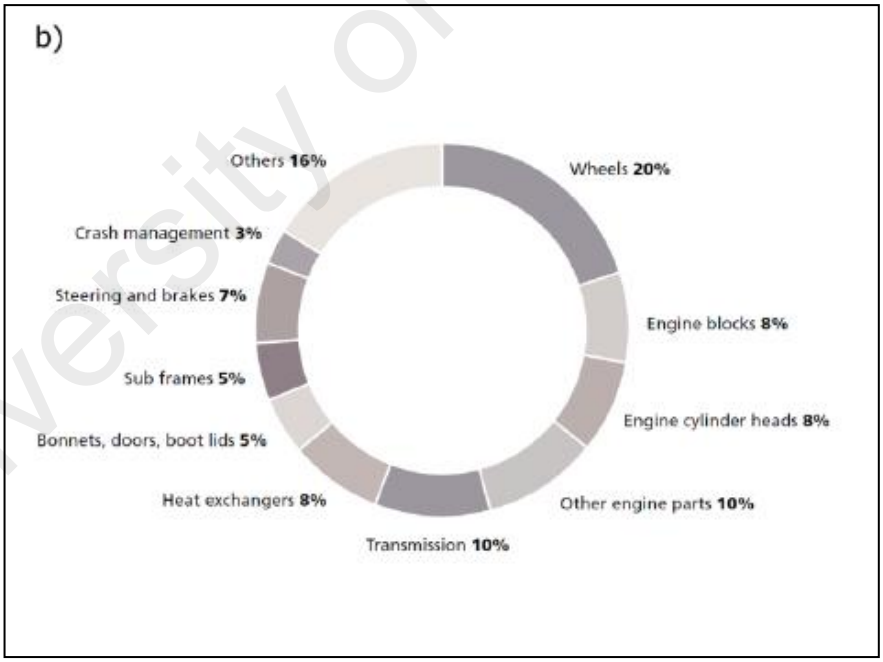

Figure 2.2: Distribution of aluminium in European cars (W.Martienssen,*et al*., 2004).

Moreover, in packaging sector, aluminium beverage cans are the main users of aluminium. Reportedly, globally 15% of aluminium consumption is comes from

aluminium cans. Corrosion resistance and protection against UV light combined with moisture and odour containment as well as the non-toxic and will not filter or spoil the products has resulted in the main use for packaging sector.

Besides that, in marine application, the aluminium extrusions and plate are used widely for superstructures of ships. The light weight property of aluminium enables marine architects to obtain better presentation from the power available by adopting the use of aluminium in the hulls of hovercraft, fast multi-hulled catamarans as well as surface planning vessels. Longer lifecycles property has made halidecks amd heldeck support structures on offshore oil and gas rigs as well as production of oil rig stair towers and telescopic personnel bridges.

Apart from marine application, building and architecture also use aluminium widely for doors, cladding, roofing, foil insulation, shop fronts, architecture hardware, windows and guttering.

Foils which made up of aluminium have thickness of 0.0065mm only. The aluminium foil is impermeable to light, volatile compounds, oils and grease, gases and water vapour. These applications include pharmaceutical packaging, insulation, electrical shielding, laminates and food protection.

2.1.3 Aluminium series, properties and applications

Aluminium alloy are subdivided into 2 main group of categories which are cast and wrought alloy. It is further subdivided into precipitation-hardenable alloys which able to be strengthened by aging and non-precipitation-hardenable alloy that only able to be improved through work-hardening only (W.Martienssen,*et al*., 2004).Elements experience hardening with the addition of further alloying elements which depends on whether the solute atom are obtainable as particles or in solid solution. Alloy hardening

is grouped into two types such as solid solution hardening (as with non-precipitation hardening, work hardenable alloys) and hardening due to elements that are originally in solid solution and are precipitating as second phases.

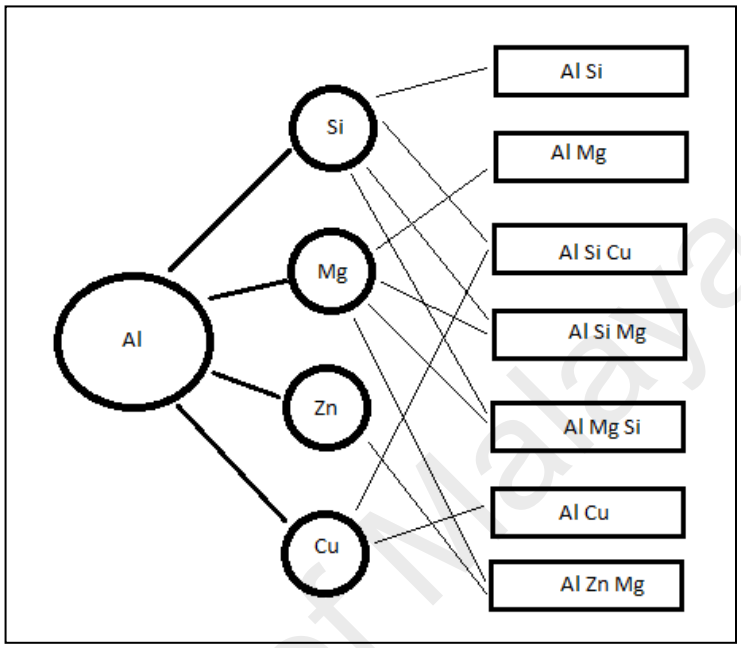

Figure 2.3: Types of casting alloy cars (W.Martienssen,*et al*., 2004).

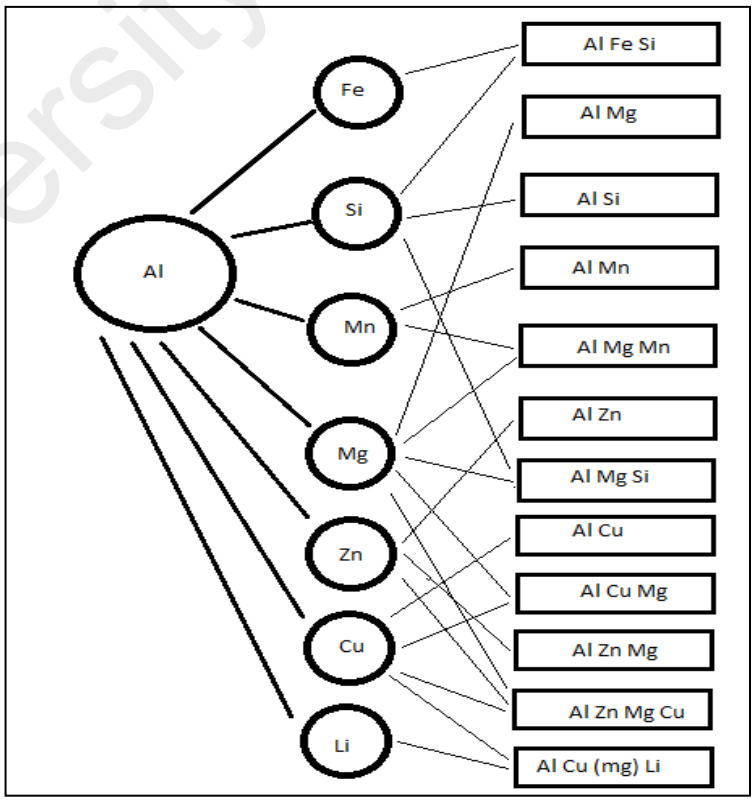

Figure 2.4: Types of wrought alloy cars (W.Martienssen,*et al*., 2004).

2.1.3.1 AA 1xxx Series

1xxx series is unalloyed aluminium which is containing dissimilar level of impurities. Iron (Fe) and silicon (Si) are the most common impurities for this particular type of series. This series consist of aluminium of purity 99% or further classification is based on the purity of the metal (Springer handbook). The 1xxx series of alloys can be strain hardened, however not recommended using if strength is the major factor to be considered. It has high electrical conductivity, formability and corrosion resistance. The typical ultimate tensile strength range between 70-185 MPa and it can be joined easily by soldering, brazing and welding.

The major applications of this series are in which the combination of tremendously high corrosion resistance and formability are necessary. For example foil and strip for chemical equipment, car truck, tank car or packaging, sheet metal work and so on. Moreover, electrical application is one of the major uses of 1xxx series because it has comparatively tense controls on those impurities that might worsen the electrical conductivity (Doty *et al*., 2003)

2.1.3.2 AA 2xxx Series

2xxx series is known as aluminium-copper alloys. The main properties of this series are heat treatable, high strength at both elevated and room temperature. Besides that, the typical ultimate tensile strength range 190-430 MPa and it can be joined mechanically as well as some alloy are weldable. They have poorer corrosion resistant to atmospheric corrosion like a number of other series and so usually are painted or clad as additional protection (Doty et al, 2003). The 2xxx series alloys typically comprises 3.5 to 5.5 wt% Cu and addition of Mg, Mn and Si and remaining Fe cars (W.Martienssen,*et al*., 2004).

It is widely used for truck body (2014) and aircraft (2024) applications, where they are used in riveted or bolted constructions. 2219 and 2048nare basically used for aerospace applications using joining methods. Some of the members in this series are even used for screw-machine stock and fasteners. Besides that, other applications includes such as heavy dump structural beams, tank trucks, trailer trucks, the booster rockets and fuel tanks of the space shuttle and internal railroad car structural members(Doty *et al.*, 2003).

2.1.3.3 AA 3xxx Series

Series 3xxx is formally known as aluminium-manganese alloys. It has good formability and moderate strength of corrosion resistance. The distinctive ultimate tensile strength recorded within the range of 110 to 285 MPa. It can also couple fairly through methods that are commercially oriented. The strength of unalloyed aluminium basically increases by the addition of manganese element in it. The chemical resistance is not spoil with the addition of the element.

The major uses of aluminium series 3xxx are chosen as materials to make cooking tools and chemical equipments due to its excellent corrosion properties. They have high corrosion resistance managing many foods and chemicals as well as in builder's hardware. Alloy 3003 is broadly applied in fabrication of sheet and tubular form for power plant and heat exchangers in vehicles due to its ease and flexibility of joining. Besides that, alloy 3004 and modified alloy 3104 are the principles for the bodies of soft drinks and beverage cans. Some other typical examples of application of 3xxx alloy series are including automotive radiator heat exchanger and tubing in commercial power plant heat exchangers. Hence, aluminium series 3xxx are extremely common used as individual alloys of system, in excess of 1.6 billion kg per annum.

2.1.3.4 AA 4xxx Series

AA 4xxx series is known as aluminium-silicon alloys. The properties of this particular series are it can be heat treated and has medium strength. The typical tensile strength falls within the range of 175 to 380 MPa. It has ability to join easily by brazing and soldering.

The primary applications of aluminium series 4xxx are used to produce forged aircraft pistons. It generates outstanding flow characteristics established by moderately high content of silicon. Second application is weld filler alloy whereby used for GMAW AND STAW structural and automotive application.

2.1.3.5 AA 5xxx Series

Series 5xxx is known as aluminium-magnesium alloys. The members of this series has properties if strain hardenable, exceptional corrosion resistance even in salt water and good toughness at cryogenic temperatures which is close to zero. It has good weldability where they can be welded directly through various techniques even thickness up to 200mm and well as has moderate strength. The typical ultimate strength falls within the range of 125 to 350 MPa.

The major application of aluminium series 5xxx is in construction and building, storage tanks, highway structures including bridges and pressure vessels, marine application and well has cryogenic tankage and systems.

2.1.3.6 AA 6xxx Series

Aluminium-magnesium-silicon alloys are broadly used wrought age-hardenable alloys. Hardening is attributed to the development of Mg_2Si phase. The uniqueness of 6xxx series has high corrosion resistance, heat treatable, outstanding extrudability and

average strength. The ultimate tensile strength is 125-400 MPa. It can be directly be welded though Gas Metal Arc Welding and Gas Tungsten Arc Welding.

Series 6xxx are used in many architectural and structural members such as railroad cars, marine frames and pipelines. Besides that, it is also used for high strength electrical bus and electrical conductor wire. Apart from that, it also used for wide-span roof structures for arenas and gymnasium.

2.1.3.7 AA 7xxx Series

Aluminium-Zinc alloys falls under AA 7xxx series. This class of alloys can be heat treated and exhibits high strength and outstanding toughness. It can be mechanically joined and the typical ultimate tensile strength is 220 to 610 MPa.

The application for series 7xxx alloys includes critical aircraft wing structures of integrally stiffened aluminium extrusions, long-length drill pipe and the premium forged aircraft part of alloy.

2.1.3.8 AA 8xxx Series

Series 8xxx known as alloys with aluminium plus other elements. The properties of this particular series include heat treatable, high conductivity, high strength with the range of 120 to 240 MPa and high hardness. The application that related to series 8xxx is used in aerospace in which it increases stiffness and reduces components weight.

2.2 Aluminium AA 3003

2.2.1 General properties of Al 3003

Table 2.2: Physical Properties of Al 3003

Properties	Value
Density	2.73 g/cm3
Melting Point	655°C
Thermal expansion	23.1*10-6/K
Modulus of elasticity	69.5GPa
Thermal conductivity	190 W/m.K
Electrical conductivity	0.034*10-6Ω.m

Table 2.3: Mechanical Properties of Al 3003

Properties	Value
Proof stress, MPa	50 min
Tensile strength, MPa	140-180
Elongation at 50 mm, %	5 min
Hardness Brinell	28 HB

Table 2.4: Chemical Properties of Al 3003

Elements	Composition %
Si	0.60 Max
Fe	0.70 Max
Cu	0.05-0.20
Mn	1.00-1.50
Mg	N/A
Cr	N/A
Zn	0.10 Max

2.2.2 Applications of Al 3003

Aluminium 3003 is widely used in many fields such as cooking tools and chemical equipments due to its dominance in many foods and chemicals handling. Apart from that, it also is used in builder's hardware due to its better-quality corrosion resistance (Doty *et al.*, 2003). With the effective addition of 1.0% to 1.5% manganese, it gives 3003 alloy a good corrosion resistance, good response to welding, cold working and forming. Thus, it is highly used in domestic electrical appliances such as washing

machines, body of cooking range and also tubes. Besides that Al 3003 also widely used in boilers and other items involving fabrication, pressing, drawing and forming.

2.3 Surface Modification

2.3.1 Surface Modification of Aluminum Alloy AA3003

Metal is the most common type of material that used in industry due its tremendous mechanical and metallurgical properties. Nevertheless, corrosion has been a major drawback for metal over a period of time as soon as it started operating. It reduces the life span of the metal and increase the cost of replacing the fault items. Thus, in order to protect the metal from corrode, few methods has been established such as apply coating, surface modification, application of inhibitors, cathodic protection and so on.

Surface modifications have been evolving rapidly in all sectors in recent days. Surface modification generally is usually done to enhance chemical, mechanical as well as materials physical properties, for instance wear resistance, corrosion resistance, biocompatibility, and surface wettability (Oshida, 2013). There are three general techniques used to modify surfaces such as add material on the surface, remove material and change the material that already present on the surface. Addition of material on the surface can be done by few methods such as evaporation, sputtering, physical vapour deposition and chemical vapour deposition. Removal of material form surfaces can be done by glow discharge treatment and sputter-etching (WC, 1992). Apart from that, modify the existing surface properties can be carried out by laser and electron beam thermal treatments. For example, ion implantation can be used to modify the coatings and surface microstructure as well (WC, 1992).

2.3.2 PVD and material coating (Zr and Si)

Physical vapour deposition technique is one of the finest methods that used in industry to deposit thin coatings on the surface (Andritschky, 1995). The corrosion protection by PVD coating has 3 parameters such as thermodynamically stability, the coating micro structure and diffusion process contained by coating and substrate. It is a high-vacuum deposition process for metals, metal alloys, or other solid chemical components using kinetic energy of ions (sputtering) or thermal energy (evaporation) to eliminate material from target and deposit it onto a substrate. Sputter coating is carried out in vacuum chamber which the target (cathode) plate is bombarded by high energy ions from glow discharge plasma in the vicinity of the target.

Zirconium is a valve metal with brilliant corrosion resistance for conditions including different types of acids, alkaline and aggressive organic solution. It has low neutron absorption coefficient but it is highly considered as biomaterial due to its electrochemical resistance and mechanical properties (Gudla,V.C.*et al.*, 2015).

2.3.2.1 Techniques of PVD

Physical vapour deposition (PVD) process is where the deposition of particles will be changed into gaseous state through physical process such as an impact process thermal evaporation. The deposition process includes three stages which are evaporation of target material (evaporation phase), transport of particles through the vacuum to the substrate (transport phase) and condensation on the substrate (condensation phase) (Hwaiyu Geng, 2005). Firstly using heating process, the kinetic energy of atoms and molecules of solid and liquid increased eventually. As the temperature increases, the separation energy and evaporation can be controlled by atoms and molecules. The evaporated particles consist mainly of atoms, molecules and cluster of different sizes and composition (K.Reichelt, 1990).

The delivery of heat for evaporation can be done by an arc discharge or laser beam, which will strike the evaporant. By the bombardment of ions whose energy is larger than 30eV, surface particles and secondary electrons will come off from target. The process is known as sputtering, at where the particles ejected, which mainly consists of atoms and molecules will be deposited on the wall of the vacuum chamber and substrate to produce the film. The average energy of ejected particles depends on the ion energy. The charged particles of the material to be deposited will be accelerated to higher energies on to the substrate and form a film. To order to obtain the homogenous coating, the structured part must move regularly or the deposition must be carried out at higher pressure. (K.Reichelt, 1990).

In order to obtain high-purity layers, it is imperative that the mean free path must be much bigger than the distance between the source and the substrate (Zant, 2014). The degree of contamination depends on the purity of the source material as well as the reaction with the residual gas in the vacuum chamber. The smaller the mean free path, the higher is the possibility of vapour particles colliding on their path between the source and the substrate.

Sputtering is a plasma process, in which noble gas ions Argon (Ar^+) are accelerated towards a target from which they eliminate particles material. There are four stages include in sputtering process which are stage one is the formation of ions through collision of inert gas atoms (Ar) with electrons and acceleration of ions towards a target, secondly eliminating of target atoms by bombardment of ions with the target and the third level known as delivery of free target atoms to the substrate. The final step is the condensation of target atoms on the substrate (Hwaiyu Geng, 2005).

2.3.2.2 Advantages of PVD

PVD process is usually useful due to their mechanical properties such as high hardness, high erosion protection and so on (Andritschky, 1995). PVD technique gives reward of accurate film thickness and smoothness control with high chemical purity, *in-situ* growth monitoring and large growth rate (Antonio Facchetti, 2004). Coating by PVD can be used on almost any type of inorganic material. It is also one of the effective methods of improving a surface's strength and durability. Besides that it also one of a safer method if compare to others as well as the process does not require extensive cleanups and it is environmental friendly. The unique advantage of PVD method is that, the fairly small deposition temperature (200-500°C), allowing most industrially significant substrate materials to be coated (Thomas Bjork, 1999). PVD method is also highly flexible in terms of film composition and microstructure offers a suitable basis for depositing continually improving coating material, with the growth of multicomponent and multilayer coatings (0. Knotek, 1993).

Table 2.5: Types of surface modification process

Method	**Strength**	**Weaknesses**	**Application**
Chemical Vapour Deposition (CVD)	Excellent conformality, economical	Residual contaminants, grain size	Intermetal dielectrics, shallow trench isolation, passivation layers, diffusion barriers
Physical Vapour deposition (PVD)	Precise control of purity and dopants	Poor conformity	Aluminium, Diffusion barriers, seed layers
Electroplating	Excellent conformality, low resistivity, economical	Limited to conductors, purity	Copper deposition
ALD	Nearly perfect step coverage	Slow	Barriers

2.3.2.3 Applications

PVD has been widely used in many fields today. PVD method used to coat the cutting tool in order to advance the cutting characteristics such as good surface finish in increase the life span of tool (Kolla Meheresh Gupta, 2018). K. Bewilogua *et al.* studied that PVD method in automotive industry to improve mechanical properties and produce hard coatings such as TiN, TiC and Al_2O_3 to increase the life time of parts. Since the mod of 1990s, PVD coatings have been used as high quality surface finish sanitary and door hardware which makes it to widely use for decorative applications.

2.3.3 Anodization

Anodization is an electrochemical process in which metals (work piece) is used as anode in an electrolytic cell to form oxide coating. This process is carried out to boost up the performance of the surface (M.G.S.Ferreira, 2012). It is a conversion process in which it has been used widely for surface finishing. Through this anodization process, the oxide layer appeared naturally to enhance the thickness and attained the desire corrosion resistance properties (P.Sahoo, 2017).

2.3.3.1 Techniques of anodization

Anodization process is the reverse process of electrolytic deposition. Upon anodizing, the work piece resembled as the anode which is known as position electrode in the electrochemical cell immersed in an electrolyte. The properties of the modification that made for the process on the sample's surface depends on the temperature of the bath and the time taken to accomplish the process. A DC electric current is passed between the sample that is made anode (positive terminal), the electrolyte and a cathode such as graphite, lead and so on. The electrolyte dissociates and oxygen is sediment at the anode when the current applied. This dissociated oxygen

reacts with substrate surface leads to formation of oxide film (P.Sahoo, 2017). The general anodizing process includes the following stages:

(i) Mechanical treatment

(ii) Degreasing and cleaning

(iii) Electropolishing

(iv) Anodizing using AC or DC current

(v) Dyeing or post treatment

(vi) Sealing

The anodized film formed consists of a thin barrier layer at the metal-coating interface and relatively thick layer of cellular structure. Every single cell consist a pore which is dependant of the type of electrolyte and experimental conditions. The quality of the anodized film determined by pore size and density (A.S.H.Makhlouf, 2011).

2.3.3.2 Advantages of anodization

High specification of metallurgically bonded finish can produced by anodization method that resists abrasion, corrosion and exposure to industrial, marine, automotive and other harsh environment. It increases surface hardness and abrasion resistance (P.Sahoo, 2017). Apart from increasing corrosion resistance, it is also enhance the durability and wear resistance of the sample upon fix into its respective application. Besides that, anodizing provides electrical insulation as the oxide later formed on the surface of the sample. It is also an excellent base or primer for secondary coating. (W.McKeen, 2006).

2.3.3.3 Applications

Aluminium anodized coatings are appropriate for outdoor applications. It has a extensive use in packaging of food and industry associates with processing. It is also

widely used in wrapping of pharmaceutical products due to its high resistance of coating to the food and pharmaceutical products (Ahmad, 2006).

2.3.4 Heat Treatment

Heat treatment is the heating and cooling of metals to alter their physical and mechanical properties, without varying its shape. It is a method of strengthening materials to improve some mechanical properties such as formability and machining. This method involves heating or cooling to high temperatures to attain the desired properties. There are few type of heat treatment process present such as tempering, annealing, normalizing, and quenching (Verardi,P. *et al.,* 1999).

Annealing is a process involves treating material to a high temperature and then cooling it very leisurely to room temperature in order to obtain microstructure with high ductility and toughness buy low hardness. The processes start with heating the sample to desired temperature and soak it for appropriate time and then closing off the furnace while leave the work piece in it. Annealing treatment depends on alloy type as well as original structure and temper. During this process, it is vital to make sure optimum temperature is achieved in portion of load, thus is advisable. The heating rate is critical thus, rapid heating is needed to prevent grain growth. The aging process involves formation of finely dispersed precipitates which include natural aging or artificial aging. This process eventually results in properties changes which basically results from formation of solute-rich microstructural domains or Guinier-Preston (GP) zones (Davis,J.R.,1993).

2.4 Nanoporous and Nanotubes

In recent days, nanoporous material has gained a great interest due to its excellent porous properties which are makes it suitable for variety of application. Many studies have been reported that to prepare unique ordered nanoporous materials, it is

better to use minerals as the inorganic sources in which it can display variety of properties from materials prepared using chemical reagents (Kiyoshi Okadaz, 2006). Nanotubes are very steady structures build up from the ring stacking of cyclic peptides. Nanotubes design can be flexible, as the outer surface functionality can be changed by varying the nature if side-chain residue (J. Banerjee, 2018).

2.4.1 Applications of nanoporous and nanotubes

Nanoporous materials with channels and cavities of molecular dimensions have a number of potential applications such as in catalysis, ion exchange, gas adsorption and so on (Materazzi, 2008). M. Koebel *et al.* provided examples of applications such as, vacuum insulation panels in which a micro or nanoporous core material that is vacuum-packaged in a metal/polymer multilayer laminate foil that gives most influential bulk insulation systems available today. The thermal conductivity is up to 10 times lesser than that of mineral wood. Apart from that, due to its high strength, nanotubes are widely used in medicinal applications (therapeutic activities) although these materials are still under study (Gaurav Verma, 2017).

2.4.2 Advantages of nanoporous and nanotubes

Due to small pores in these materials, discrimination between molecules and ions based on sizes and shapes is possible, while the confines environment enhances chemical reactions (M.G. Debije, 2016). Nanotubes have very high range of electrical conductivity and good strength (Gaurav Verma, 2017). Even though they are known as low cytotoxic and more biocompatible, nanotubes do not show any side effects (Nadine *et al.*, 2004).

2.5 Al_2O_3 Nanoporous

2.5.1 Properties of Al_2O_3

The decorative appearance, mainly of the transparent and clear anodic porous alumina film formed as a great surface finisher, architects and designers. This porous nanostructure is optically transparent, electrically insulating, semi-transparent, chemically stable, biocompatible material and a bio-inert material (Gerrard Eddy Jai Poinern, 2011). Apart from the appearance, anodized Al also enhanced the mechanical and tribological properties as well as improved corrosion resistance (Gudla, V.C. *et al*., 2015). The properties are:

Table 2.6: Properties of Al_2O_3

Properties	**Description**
Hardness	65 to 70 Rockwell C, 850-900 HV/10
Colour	Clear transparent to ceramic off-white
Coating Thickness	A few μm to approximately 200 μm
Dielectric	Non-conductive and will withstand 800V per 0.001" thickness
Machining	Can be ground, lapped, honed or polished.
Dyeing	Dye by most colours
Resistivity	Between 10^6 to 10^{12} Ohm-cm

Table 2.7: Properties of porous Al_2O_3 (Isobe,T *et al*., 2006)

Property	**Value**
Density	2.47 g/cm^3
Relative density	62%
Open porosity	36%
Closed porosity	2%
Pore size	14 μm
Pore number density	1700 pores/mm^2
Pore area (perpendicular)	25.3%
Pore area (parallel)	41.0%
Three-point bending strength	171 ± 19Mpa
Weibull modulus	9.28
Young's modulus	132 GP

2.5.2 Formation and growth mechanism of Al_2O_3

Anodising aluminium is a controlled oxidation process where oxide layer is formed in which results in aluminium oxide. It is usually performed in electrochemical cell, where the aluminium (work piece) is the anode and graphite or Pt shall be cathode. A standard self-organized porous nanostructure produced through anodizing process. The porous nanostructure Al_2O_3 formation has controllable variables such as acid type, concentration of electrolyte and voltage applied. The electrolyte used is based on a mixture of oxidizing inorganic acids, which also acts as charge carrier (Gudla,V.C. *et al.*, 2015). The overall anodizing process can be described as:

Anodic reaction at metal-interface: $2Al + 3O^{2-} \rightarrow Al_2O_3 + 6e^-$

Anodic reaction at the oxide-electrolyte interface: $2Al^{3+} + 3H_2O \rightarrow Al_2O_3 + 6H^+$

Cathodic half reaction: $6H^+ + 6e^- \rightarrow 3H_2$

Overall anodizing reaction: $2Al + 3H_2O + 2Al^{3+} + 3O^{2-} \rightarrow 2Al_2O_3 + 3H_2$

The depth of the barrier layer is affected by the concentration of electrolyte and the applied anodising potential. The barrier layer thickness remains constant during growth of porous anodic film (Gudla, V.C. *et al.*, 2015).

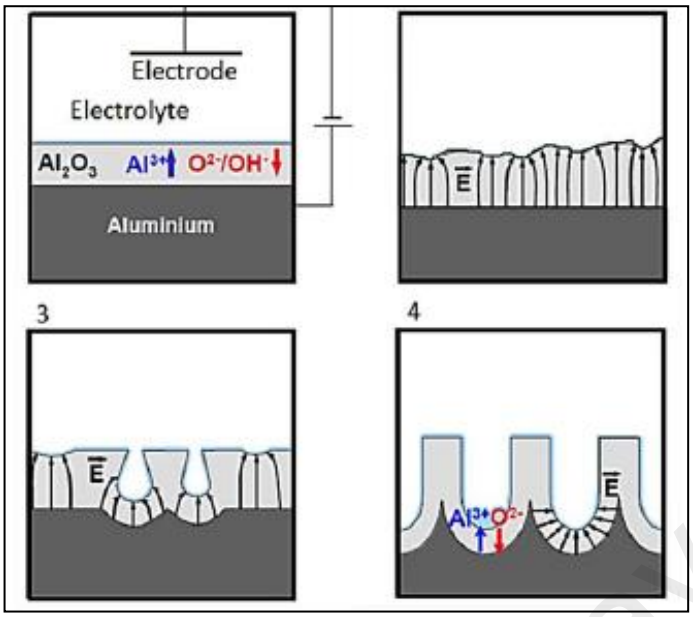

Figure 2.5: Schematic diagram showing pore development during anodizing of Al in acid electrolyte (Gudla,V.C. *et al.*, 2015).

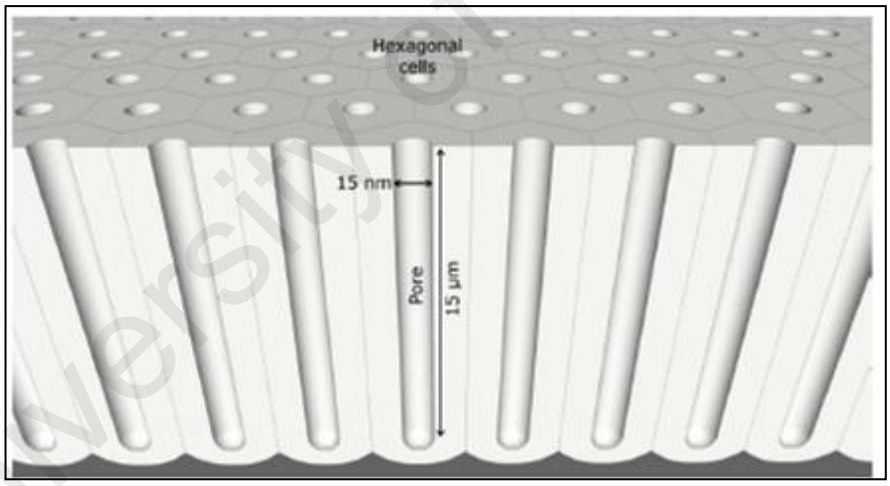

Figure 2.6: The ideal structure of a porous anodic layer (Gudla,V.C. *et al.*, 2015).

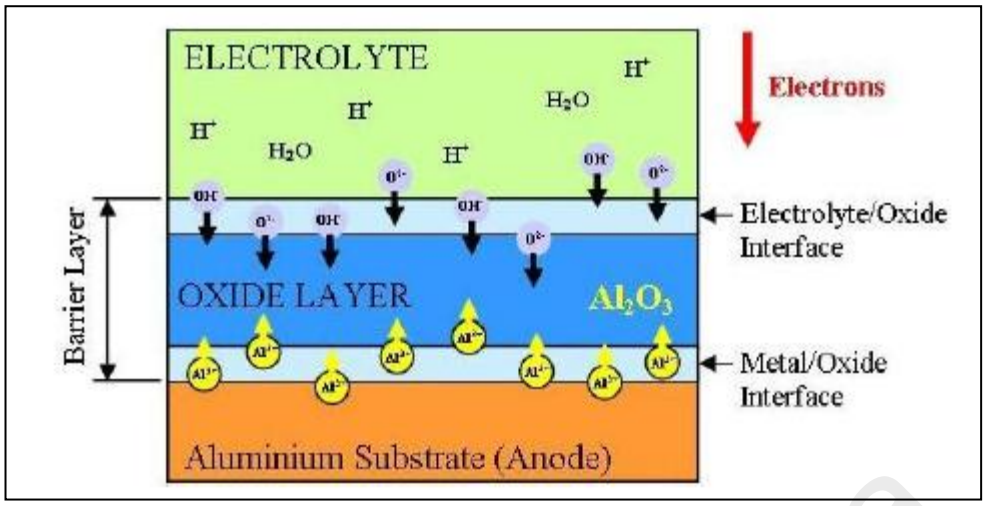

Figure 2.7: Schematic of formation of the barrier layer (Gudla,V.C. *et al*., 2015).

2.5.3 Applications of Al_2O_3

Most of the anodized aluminium is used in various industries which includes decorative surfaces displaying pleasing aesthetics, corrosion resistance surfaces, surfaces with high hardness for increased wear resistance, improved adhesion of top organic paint coats and functional surfaces with tailored dielectric and optical properties (Gudla,V.C. *et al.*, 2015). In aerospace industry, aluminium is anodized in chromic acid produces an oxide layer which provides an useful surface treatment prior to painting. Apart from that, current studies have shown that nanowires or nanotubes have potential to make a role for envelopment of electronic devices and computer system (Gerrard Eddy Jai Poinern, 2011).

Alumina also widely used in automotive industry such as in combustion engines. For reciprocating engines it used as valve guide, cam follower rollers, thermal barrier coatings in exhaust pipes, ball bearings, pump seals and spark plug insulators whereas for turbine engines alumina is used in nozzles, ceramic lining of combustors and turbine blades.

Moreover, porous alumina widely used in industry such as optical biosensing platform, optofluidic application, electrochemical sensors for biomedical and environmental analysis. Apart from that, porous alumina also intended to widen the field to drug delivery and biomedical applications including dental implant, orthopedic, heart, coronary, vasculature stent, immunoisolation, skin healing, tissue engineering and cell culture (Losic,D *et al.*, 2015)

2.6 ZrO_2 and SiO_2 nanotubes and their applications

Silica nanotubes are extremely resistant to acidic pH and faster dissolution rate is achieved at pH. This degradation pattern shows that the silica nanotubes are exceedingly preferable for oral drug delivery which could overcome harsh acidic environment (Pragasam Viswanathan, 2017). Besides that, the nanotubes dissolution can be changed based on the thickness of the silica nanotubes (Hu *et al.*, 2010).

Zirconia nanotubes are widely used in biomedical applications especially in bone implant integration due to its high flexural strength, fracture resilience and other chemical properties. It is a ceramic of white colour appearance which makes it a suitable material for patients with metal ion sensitivity (Sweetu B. Patel, 2017). Besides that, zirconia also is used to manufacture punches and dies for use in tableting machines. It needed low work to control die wall friction during ejection (Alpagut Kara, 2004).

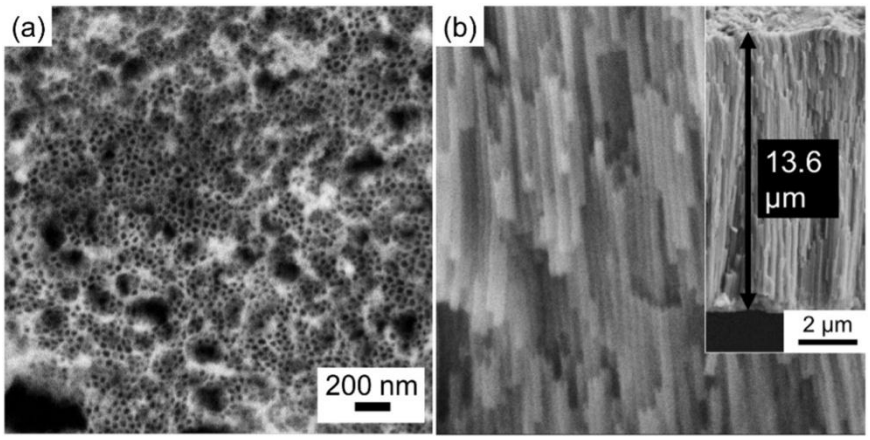

Figure 2.8: FESEM images of as-anodized ZrO_2 nanotubes array (Nurilhuda Bashirom, 2017).

2.7 Adhesion

Adhesion is the bond strength measurement of a coating to a substrate. When a coating applied on a substrate, their mechanical, physical and chemical properties will be altered as well. Hence, the adhesion strength between the coating and substrate can be measured using scratch test method. Scratch test is a practical method for attaining relative, rather than fixed values of adhesion strength for coating applied on substrate. Scratch testing is a straightforward, semi-quantitative technique that used to determine the adhesion strength (Dunstan Barnes, 2012). The advantages of adhesion test is that it simulate the usage stress condition which is more strictly resembles tensile adhesion strength testing. Furthermore, it is also used to measure the adhesion of thin coatings without the threat of bonding agents penetrating the coating. Scratch test involves applying a normal force to the surface of a sample through a stylus while the stylus is displaced relative to the sample at a constant speed (Valli *et al.*, 1985). Besides that, the critical load is the force used in which the coating fails and it can be used as comparative study for adhesion strength. Thus, if the coating-substrate adhesion is good, the buckling should spread through the coating, where as if the adhesion strength is poor, the buckling should propagate at the coating-substrate interface (Dunstan Barnes, 2012).

2.8 Microhardness

Microhardness testing is a method of identifying the material's hardness or resistance to penetration when test samples are small or thin. An indentation is made on the specimen by a diamond indenter with the application of load. Basically, it was comprehensive to research studies of individual phases, orientation effects in single crystals, diffusion gradient, aging phenomena and so on for both metallic and ceramic materials (R.E.Smallman, 2014). In microhardness testing, typical load are in the range of 1-100gf. The hardness result that obtained from the testing portrait the ability of the item to resist additional deformation with respect to applied load (P.bhattacharya, 2014).

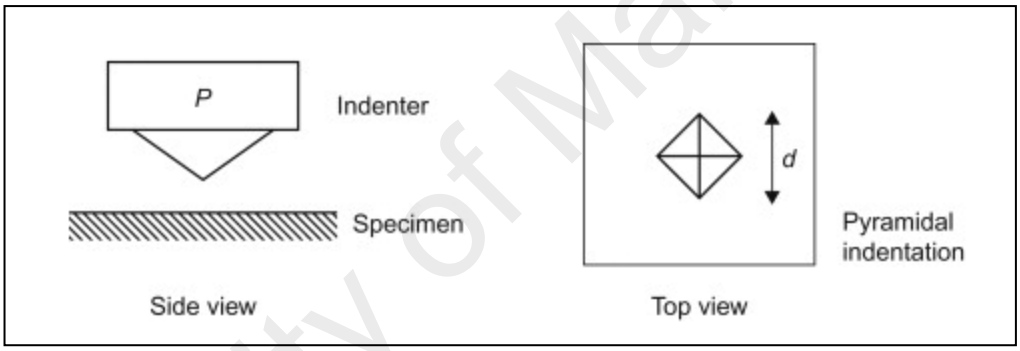

Figure 2.9: Microhardness test method (R.E.Smallman, 2014)

There are several factors that manipulate the selection of hardness test such as the size and shape of workpiece, the extent of flatness of workpiece, the hardness range of the material that being tested, the surface state of the workpiece and the characteristic of indentation mark (B.Raj, 2016).

2.9 Corrosion behaviour of Al

2.9.1 Corrosion behaviour of Aluminium (Al)

In general, aluminium has good corrosion resistance especially in atmosphere due to its natural oxide layer. However, corrosion in metal is an electrochemical reaction which involves oxidation of anode into positive ion, which is released from

solid metal. The oxidation is coupled with a reduction reaction. For example, in the case of a system aluminium and water, the metal is anode and the water is electrolyte. Cathodic reaction is common in the system are reduction of hydrogen ions to hydrogen and reduction of oxygen to either hydroxide (in alkaline or neutral environment) or water (in acid environment). The oxidized aluminium results in Al $(OH)_3$, which is insoluble in water and precipitate as a white gel.

Oxidation : $Al \rightarrow Al^{3+} + 3e^-$ (2.1)

Reduction : $2H^+ + 2e^- \rightarrow H_2$ (2.2)

: $O_2 + 2H_2O + 4e^- \rightarrow 4OH^-$ (2.3)

: $O_2 + 4H^+ + 4e^- \rightarrow 2H_2O$ (2.4)

Forming of corrosion product: $Al^{3+} + 3OH^- \rightarrow Al(OH)_3$ (2.5)

Aluminium is unexpectedly resistant to corrosion taking into account its low electrode potation. The standard electrode potential of aluminium is -1.68V. The more the electronegative potential of a metal, the easier for it to oxidize but the potential is depends on the system (Gustafsson, 2011).

2.9.2 Corrosion behavior of nanotubular structure

Aluminium has an oxide layer (Al_2O_3) on the surface which powerfully control electrochemical behavior. The oxide layer formed instinctively, thus it is naturally passivated by water and oxygen in the air. In water, the natural aluminium oxide is unbalanced. The oxide films tend to grow and experience some modification when present in water (Gustafsson, 2011).

Zirconia is an attractive material since it offers high chemical stability, mechanical strength and temperature resistance. This zirconia has high transparency and refractive index, oxygen-conductive membranes, catalyst supporter and also

anticorrosion barrier coating, it gives high protection against environment corrosion (Pareja.R *et al., 2103*).

2.10 Wettability

Wettability is the capability of a liquid to uphold contact with a solid surface, and it is restricted by the balance between the intermolecular interactions of adhesive type (liquid to surface) and cohesive type (liquid to liquid). The wettability can be evaluated by contact angle. When the contact angle is smaller than 90°, the wettability is considered good whilst wettability is identified as poor when the contact angle is larger than 90. The contact angle can be affected by various factors such as physic-chemical properties which is include chemical reaction between liquid alloy and solid oxide. Apart from that, oxygen partial pressure and crystal structure of oxide phase as well as surface roughness of solid oxide also may affect the contact angle result (Toshihiro Tanaka, 2014).

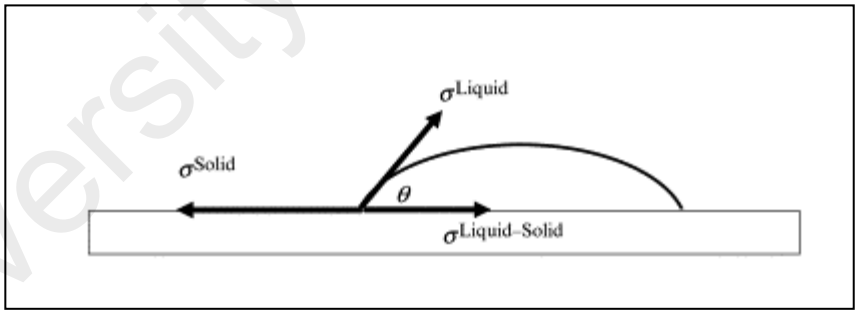

Figure 2.10: Contact angle during wettability (Toshihiro Tanaka, 2014)

CHAPTER 3: METHODOLOGY

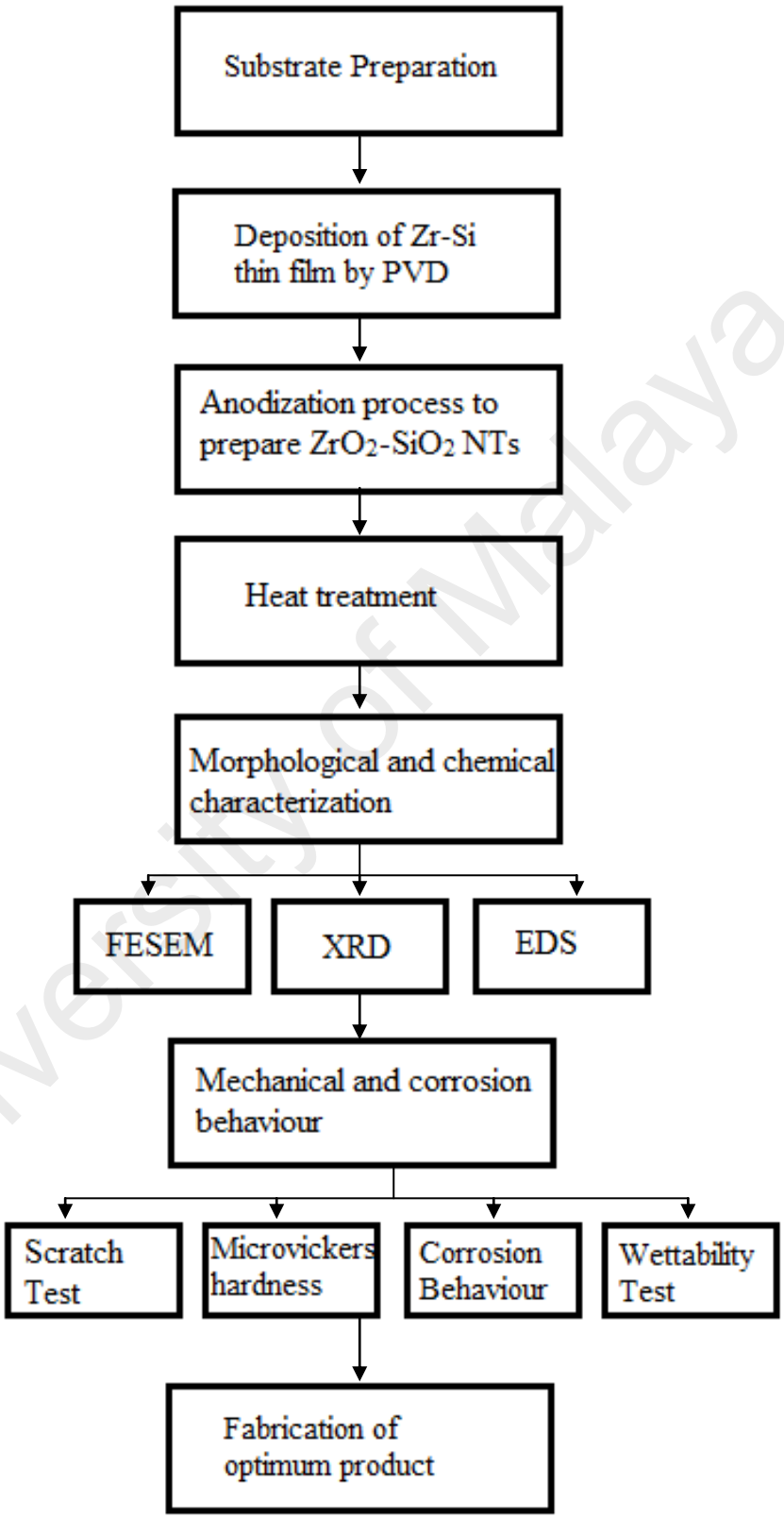

Figure 3.1: Flowchart of methodology

3.1 Substrate Preparation

The aluminium alloy series 3 substrate plates with dimensions of 15 mm × 15 mm × 2 mm fabricated from KAMCO ALUMINIUM SDN BHD, Kuala Lumpur, Malaysia. Once the desired dimension of the substrate prepared by using wire cut machine, the samples were then grounded by silicon-carbide emery papers ranging from 800-2400. The substrates then continued to polish by using diamond slurry suspension to get a mirror finishing. Sonication in acetone at temperature of 40°C for duration of 10 min was carried to remove any impurities left behind on the surface of the substrates. Upon the completion of sonication process, the substrates were then cleaned several times by using distilled water and continued by drying the samples at temperature of 100°C for duration of an hour before deposit Zr-Si thin film on the surface of the substrate.

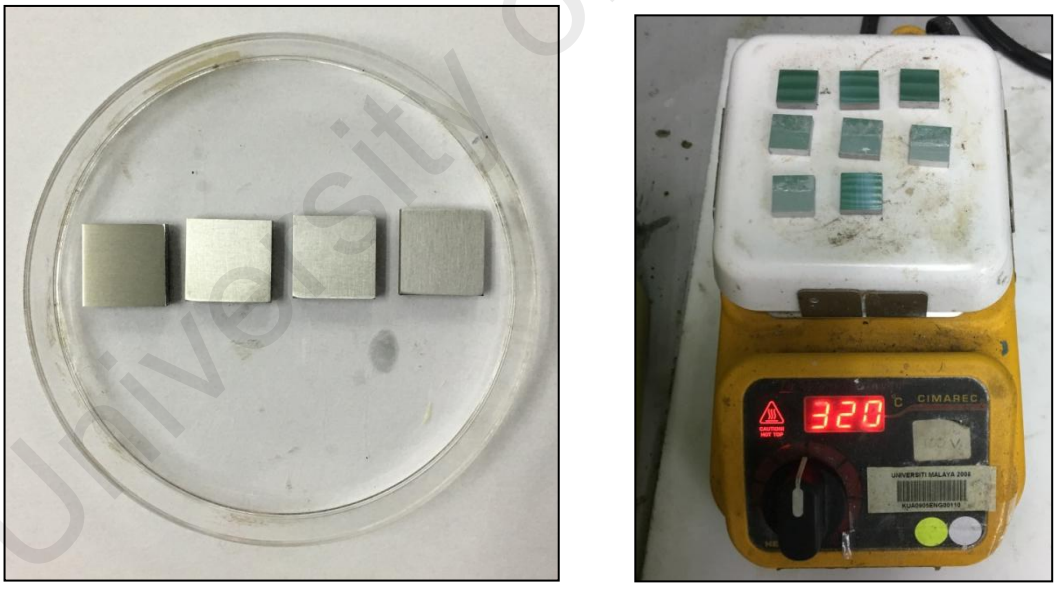

Figure 3.2: Substrate preparation

3.2 Deposition of mixed Zirconium-Silicon thin film

Physical vapour deposition (PVD) Magnetron sputtering method was used to deposit target of pure mixed zirconium (Zr, 99.995% purity) and the silicon (Si, 99.995% purity) thin film on the surface of substrate by using SG Control Engineering PteLtd. series machine. The substrate and target was placed in a fixed distance of 150 mm. Before the targeted ion deposited on the substrate, at first the target was pre-sputtered in argon environment to eliminate the oxide layer and the chamber was evacuated below 5.2×10^{-5} Torr. The detail of the parameters which used for PVD coating process is as summarized in Table 3.1.

Table 3.1: Factors and parameters used in the experiment.

Parameter	Silicon target	Zirconium target
Power (W)	150 (RF)	300 (DC)
DC bias voltage (v)	0	75
Working pressure (Torr)	2.666×10^{-3}	2.666×10^{-3}
Argon gas flow rate (sccm)	20	20
Time (h)	2	2
Temperature (◦C)	200	200

Figure 3.3: Deposition of Zr-Si thin film using PVD method

3.3 Preparation of mixed oxide ZrO_2-SiO_2 nanotubular arrays

ZrO_2-SiO_2 nanotubular arrays were formed by using anodizing method. Anodization method was conducted through a two-electrode electrochemical cell in which aluminium substrate placed on anode and graphite rod with a diameter of 7mm positioned in cathode. The distance both anode and cathode electrodes are maintained at 20 mm. The experiment was conducted at 60V for 30 min and 1 h in an ammonium fluoride (NH_4F, Sigma-Aldrich CO., 0.5 wt%) electrolyte dissolved in a 95/5 glycerol (g,Baker CO.) and distill water solvent mixture at room temperature by using direct current (DC) power source (Model E3641A, Agilent Technologies, Palo Alto, USA). Once the anodization is completed, sample is then taken out and cleaned with distilled water to eliminate any impurities from the surface. Lastly, the anodized samples were heat treated at temperature of 500, 600 and 700°C for duration of 1 h under normal atmosphere. The heating and cooling rate is at 5 °C/min.

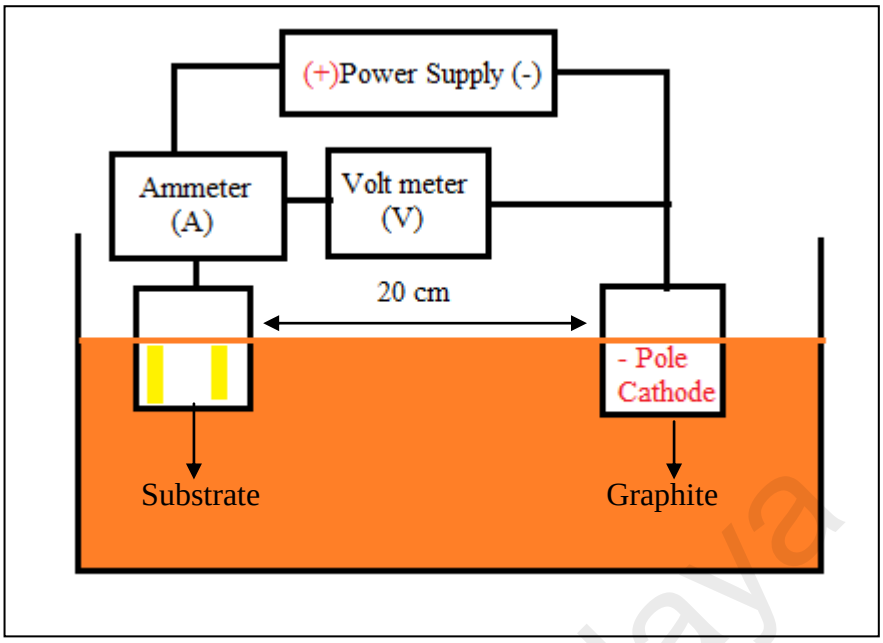

Figure 3.4: Schematic view of the anodization process to produce mixed ZrO_2- SiO_2 nanotubular arrays

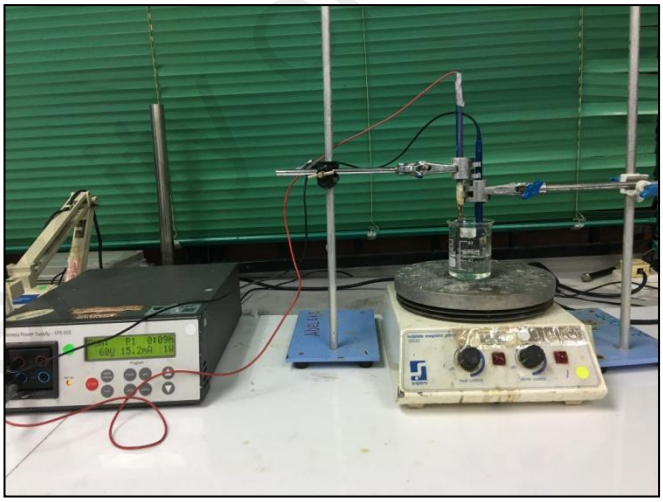

Figure 3.5: Anodization process setup

3.4 Phase analysis and Microstructural Characterization

The surface characterization of the deposited thin film on the aluminium substrate was investigated by using a field emission scanning electron microscope (FESEM, SU8000, Hitachi, Japan) with an acceleration voltage of 1 to 2 kV. The cross sections of samples were cut into desired dimensions by using high precision cutter set

with diamond blade for sample preparation. Energy dispersive X-ray spectrometry (EDS) is used to determine the atomic concentration and the two-dimensional distribution of the elements. Moreover, the composition of the phases and purity of the substrates, mixed zirconium silicon, ZrO_2 SiO_2 nanotubular arrays and annealed samples were analyzed by X-ray diffractometry (XRD; Philips PW1840, the Netherlands) with Cu Kα radiation (λ=1.54178 Å) functioning at 45 kV and 30 mA, 2 theta range of 30°-80°, scan rate of $0.1°.s^{-1}$, and step size of 0.026°. The XRD patterns were checked with the aid of "*PANalytical X'Pert HighScore*" software wherein all the reflections were equated with the standards gathered by the Joint Committee on Powder Diffraction and Standards (JCPDS, card #005-0682).

3.5 Adhesion strength

By using a Micro Materials Nano Test (Wrexham U.K) which is equipped with a diamond indenter, the adhesion strength of the deposited thin film able to be calculated quantitatively. The radius and angle that used was 25.0 ± 2.0 μm and 90.0 ± 5.0° respectively. The testing was carried out with a velocity of 5 mm s^{-1} and load rate increased up to 9.2 mNs^{-1}. The scratched specimens' surfaces were analyzed under a light optical microscope (Olympus BX61, Tokyo, Japan). Thus, the adhesion strength is defined as total coating failure, in which specimens were placed perpendicularly to scratch probe while the contact was remained static. The test was closely monitored throughout the testing period. In order to access the baseline sample topography, a pre-scratch scan was conducted using an ultra-low contact force. The scratch test was run for three times according to the required load using diamond indenter.

The specimens were further investigated by performing scratch hardness test on the mixed Zr Si thin film after PVD and ZrO_2 SiO_2 nanotubular arrays after heat treatment. This was conducted to determine coating resistance to plastic deformation

under the motion of a single point (stylus tip) and associates with various combinations of surface properties because the indenter moved tangentially along the surface. It is a great technique to measure the damage resistance of a material. This can be used for materials such as metals, alloys and selected polymers. It is according to the measurement of residual scratch width, after the stylus is removed to generate the scratch hardness number. Hence, it reflects the plastic deformation as a consequence from the scratch and not the immediate state of mixed elastic and plastic deformation of the surface. The magnitude of the scratch hardness number is determined by both the stylus tip radius and the normal load. This is because the level of stress at the stylus tip is a will affect contact geometry and applied force. In order to obtain the scratch hardness number, calculation is made by dividing the applied normal force on the stylus by the projected area of the scratch contact. Assumption is made that hemispherically-tipped stylus produces a groove whose leading surface has a radius of curvature *r*, the tip radius of the stylus. The final scratch width is the diameter that extracted from the projected area of the contact surface. The critical load is defined at the onset of the coating loss, which is associated with the appearance of the metallic substrate inside the scratch channel. This measurement was carried out using optical microscope. The frictional coefficient at the critical load was obtained by using the tester (Ruckh et al., 2008, ASTM, 2003, Jaworski et al., 2008). The scratch hardness HS_p was evaluated by applying the specification of ASTM G171-03 norm:

$$HS_P = \frac{8P}{\pi w^2} \qquad \text{Eq. (1)}$$

Where HS_p, P and w are the scratch hardness number, normal force and the scratch width, respectively.

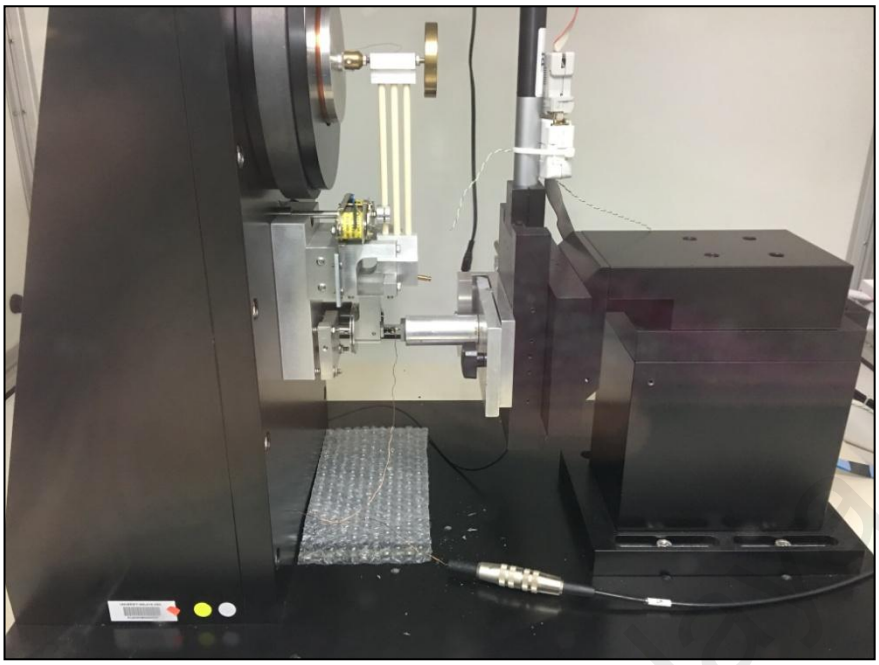

Figure 3.6: Scratch test

3.6 Microhardness

Vickers microhardness testing machine (Mitutoyo-AVK C200-Akashi Corporation, Kanagawa, Japan) was used to determine the microhardness value of the sample. The testing was carried out with the load of 98.07 mN. The allocated dwell time is 15 s at room temperature. The single point and average points were determined by indenting 5 times per sample.

3.7 Corrosion studies in sea water

Potentiodynamic polarization measurements carried out using a standard three-electrode configuration which is working electrode, counter electrode and reference electrode. In this experiment, reference electrode that has been used is saturated calomel electrode (SCE), graphite as counter electrode and aluminium samples as working electrode.

The electrolyte that used throughout the entire experiment was artificial sea water. The artificial seawater prepared in the room temperature. According to the

Burkhoder's formulation B, the compositions of the simulated seawater were as follows (per liter):23.476 g NaCl+3.917 g Na_2SO_4+ 0.192 g $NaHCO_3$+ 0.664 g KCl+0.096 g KBr+10.61 g $MgCl_2.6H_2O$+ 1.469 g $CaCl_2.6H_2O$+0.026 g H_3BO_3+ 0.04 g $SrCl_2.6H_2O$+0.41 g $MgSO_4.7H_2O$+ 0.1 g NH_4Cl+ 0.1 g $CaSO_4$+ 0.05 g K_2HPO_4+0.5 g tri-sodium citrate+ 3.5 g sodium lactate+ 1 g yeast extract. The pH was adjusted to 7.5 ± 0.1 using a 5 M NaOH solution (Yuan et al., 2013).

The surface area that exposed into the electrolyte was $1cm^2$. A potentiostat Bio-Logic SP-150 monitored by a PC computer and EC-Lab software were used to collect and evaluate the experimental data. The potential range from -2000 to +2000mV versus SCE reference electrode shall be recorded in the potentiodynamic polarization curves. The scan rate that was used during the experiment was $1mVs^{-1}$. 30 seconds were applied at the beginning of the experiment to allow the testing develop its steady-state. The testing repeated in same conditions a few times to verify the consistency of the results that obtained.

As the experiment completed, the Tafel plot obtained. From the Tafel plot, it could possible to extract important information such as corrosion current (I_{corr} / μA cm^{-2}) and corrosion potentials (E_{corr} / V_{SCE}). The corrosion protection efficiency (*P.E.*) was also estimated using the following equation (Yu et al., 2014):

$$P.E.(\%) = \frac{I_{corr}^{0} - I_{corr}^{c}}{I_{corr}^{0}} \times 100 \qquad \text{Eq. (3)}$$

Where I_{Corr}^{0} is the corrosion current of the bare series 3 and I_{Corr}^{c} is the corrosion current of the coated sample.

Moreover, *CR* was calculated by the following formula:

$$CR(mmyear^{-1}) = \frac{0.13 I_{corr}(E.W.)}{d} \quad \text{Eq. (4)}$$

Where *E.W.*, *d*, and I_{corr} are equivalent weight of the corroding species in g, density of the corroding species in g cm^{-3}, and corrosion current in A cm^{-2}.

3.8 Surface Wettability

By using a video-based optical contact angle measuring system (OCA 15EC, Data Physics Instruments GmbH, Germany), the surface wettability (hydrophilicity) of the samples was obtained. The deionized water deposited on the specimens' surface to measure the contact angles of the drops in order to obtain the result. To evaluate the contact angle of the specimens, a constant liquid volume of 5 µl was used. The parameters that used to carry out the experiment were drop velocity of 2 µl s^{-1} at a temperature of 26±1 °C. To calculate the contact angle "θ", the droplet height "*h*" and width "*d*" were measured as follows (Elias et al., 2008):

$$\theta(^{\circ}) = 2\tan^{-1}\left(\frac{2h}{d}\right) \quad \text{Eq. (5)}$$

CHAPTER 4: RESULT AND ANALYSIS

4.1 XRD Analysis

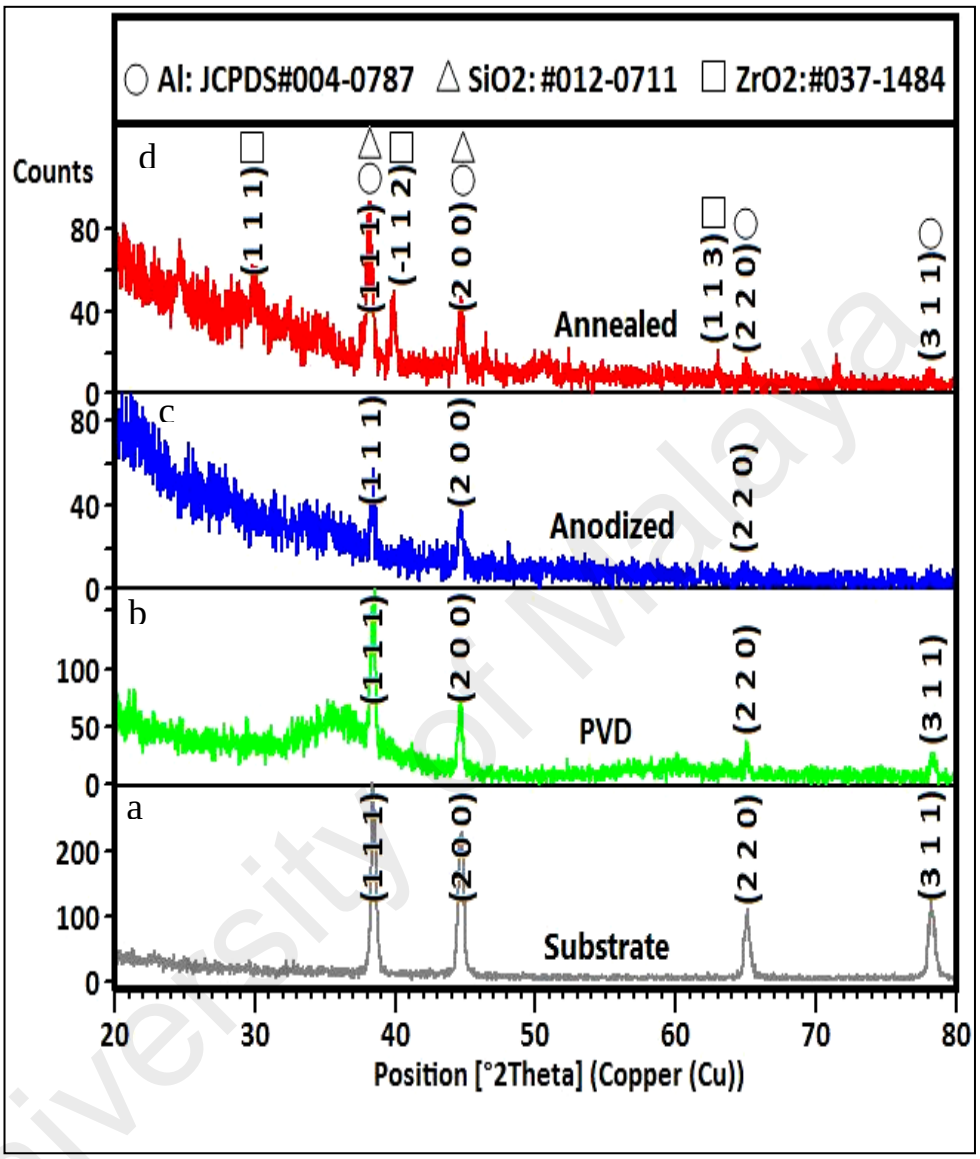

Figure 4.1: XRD profiles of the (a) substrate, (b) PVD coated sample, (c) anodized sample and (d) annealed sample at 500 °C for 1 h.

Figure 4.1 illustrate the substrate Al, AA3003, deposited target material (Zr-Si) by PVD, anodised ZrO_2-SiO_2 nanotubes and annealed sample at 500 °C for an hour in XRD profiles. Figure 4.1(a) illustrates that the XRD reflection of substrate showed peaks at 2ϑ= 38.5°, 44.5°, 65.0° and 78.5 which are related to the (111), (200), (220) and (311) planes, respectively. Figure 4.1 (b) showed the 2θ appeared to be the same as

substrate in figure 4.1 (a), however, the intensity of the peaks has been reduced due to the PVD deposition of silicon and zirconium on the surface. Figure 4.1 (c) showed the intensity of the peaks reduced even more and the result could be overlap between silicon, zirconium and aluminium. However, the annealed specimen results showed some additional peaks such as 2θ= 28.5°, 40.0° and 62.5° in related to (111), (-112) and (113) planes, respectively. These are characteristic peaks of ZrO_2. In addition, some characteristic peaks of SiO_2 are also observed which overlapped with Al reflections. This is because, after annealing process the oxide layer of zirconium and silicon become more revealing and visible for analysis. Hence, the peaks in figure 4.1 (d) showed the presence of both ZrO_2 and SiO_2 in the annealed sample. Thus, XRD results clearly indicated that a mixed oxide structure was formed after annealing of the anodized sample.

4.2 FESEM images and microstructural Analysis

Microstructural analysis was carried out by using Field Emission Scanning Electron Microscopy (FESEM) to study the morphology of the modified AA 3003 surface. Figure 4.2 shows the image which was taken on the surface of substrate without any surface modification. The surface shows bare look of the substrate after polished by using the suspension under 2 μm magnification. Figure 4.3 shows the surface of Aluminium AA3003 after 5 h of PVD process. The deposited thin film shows very smooth surface with relatively smaller grains. Moreover, Figure 4.3 shows no presence of pits or pinholes as well as agglomeration of grains on the surface. Thus, the mixture of Zr-Si was perfectly carried out under optimized PVD conditions and parameters.

Figure 4.4 shows images of the anodized sample at duration of 1 hour, with applied DC of 60V in an electrolyte containing 38 mL of glycerol + 2 mL of water + 0.2341 g of NH_4F. The anodization process begins with small irregular pits due to the dissolution of oxide layer which then further developed in to larger pores. With a prolonged anodization time of 1 hour, more uniformly distributed mixed ZrO_2-SiO_2 nanotubes were formed on the surface of modified AA3003 substrate. During the anodization process, the thickness of the oxide layer also increases which gives impacts on the pore sizes and density. The widening or growth and propagation of the pores take place due to internal movement the interface of thin oxide layer and metal substrate. As a result, oxide particles in hollow cylindrical geometry are developed into nanotubular structure. Hence, this feature is an important parameter that contributing for a good corrosion resistance properties. According to previous study, the electrolyte that used for anodization is moderately stirred during experiment. Either water-based or organic based electrolyte was used to put the length of tubes in control (D.Regonini., *et al*., 2010).

Furthermore, to enhance the adhesion of mixed ZrO_2-SiO_2 NTs, heat treatment was carried out at a heating and cooling rate of 5 °C min^{-1} at temperature of 500 and 600 °C respectively for duration of 1 h under atmospheric condition. The analysis of FESEM for annealed NT's at 500 °C is demonstrated in Figure 4.5 (a). The image at 500 °C shows highly oriented arrays of ZrO_2-SiO_2 nanotubes were formed and the structure is still intact perfectly. Whereas, samples that annealed at temperature of 600 °C is shown in Figure 4.5 (b) the structure has severe changes and believe to be collapsed during the heat treatment. From the cross sectional image in Fig. 4.6, the average coating thickness of the Zr-Si thin film and ZrO_2-SiO_2 are around 3 μm and 360 nm, respectively. In a previous study, it has mentioned that during annealing the nanotubes grown at 450 to 500 °C in glycerol. It has also mentioned that with increase

in annealing temperature, the crystallization of the substrate disturbed the tubular architecture causing collapse and sintering of the structure which explains the situation as showed in figure 4.5 (b). At higher annealing temperature, rutile appears 500-550 °C and becomes the dominant phase at 600 °C (D.Regonini., *et al*., 2010).

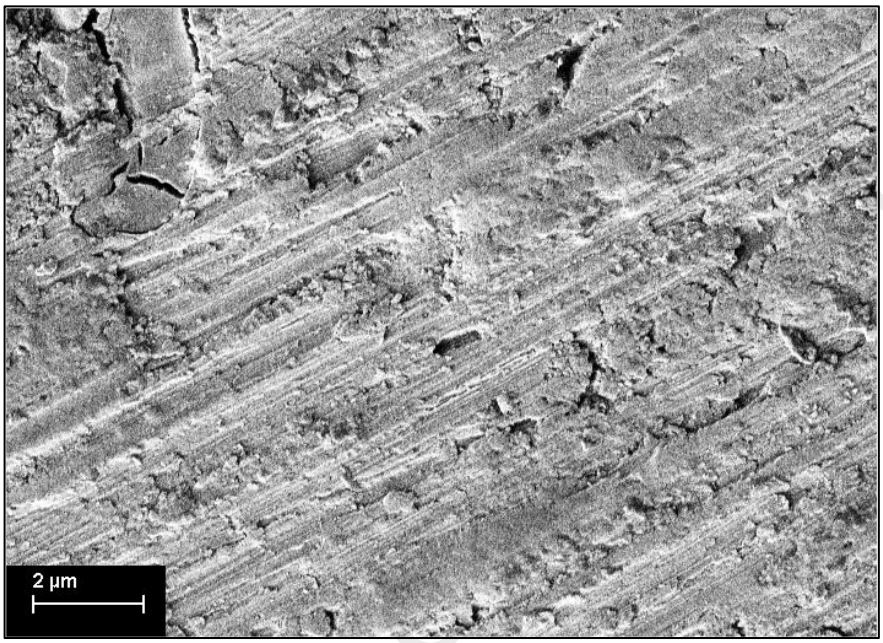

Figure 4.2: Top View FESEM images of AA3003 as substrate

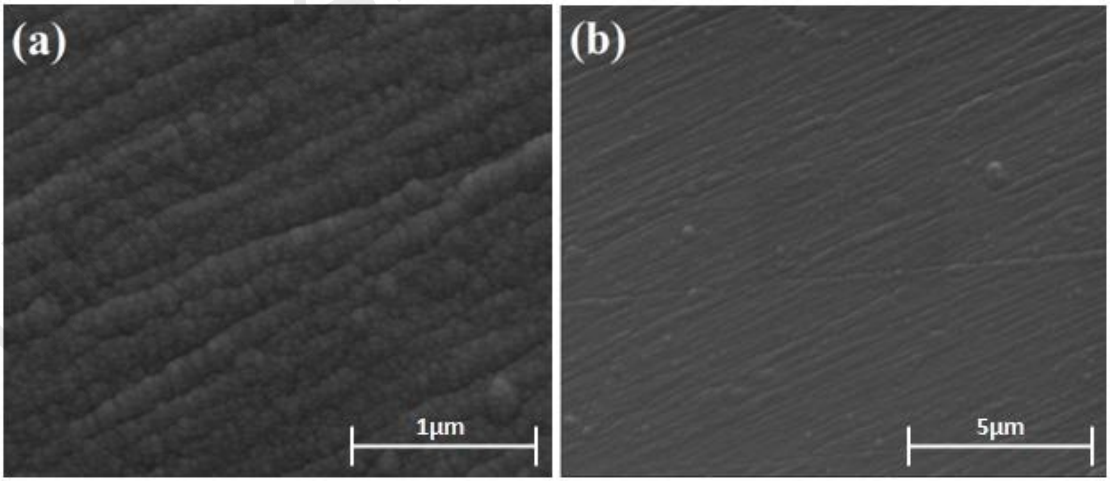

Figure 4.3: Top View FESEM of (a, b) Zirconium-Silicon thin film after PVD at different magnification

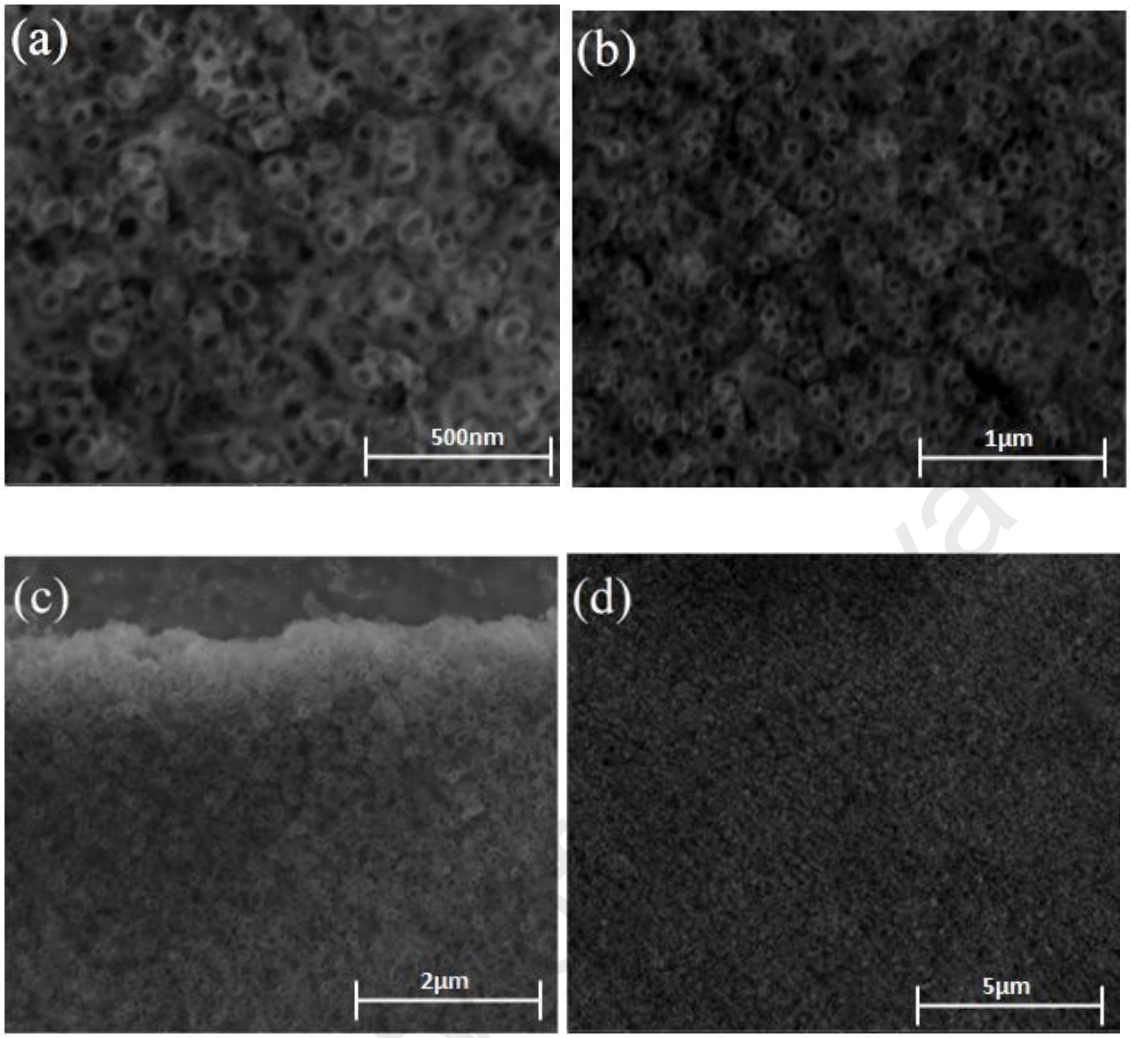

Figure 4.4: Top view FESEM images of ZrO_2-SiO_2 nanotubular arrays after anodization at different magnification

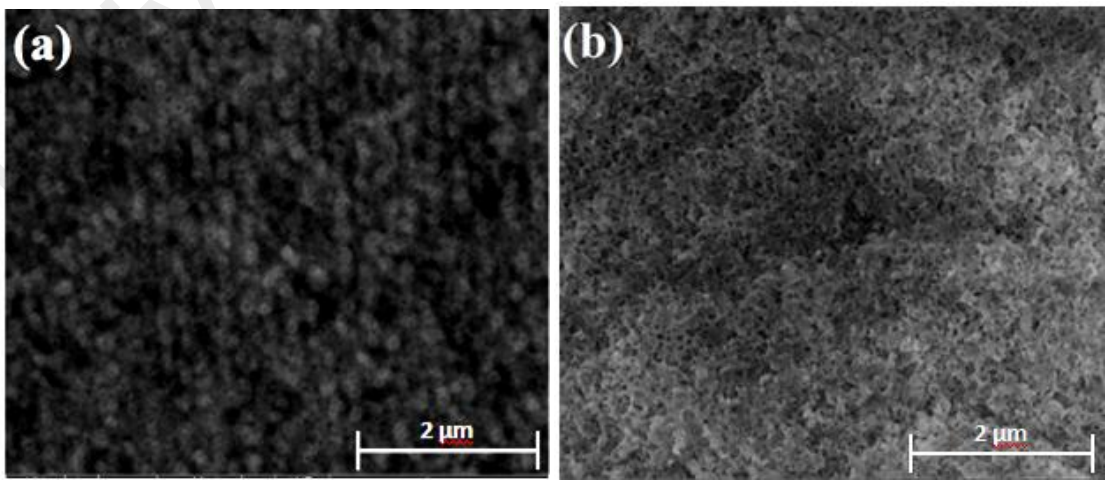

Figure 4.5: Top view of FESEM images of ZrO_2-SiO_2 nanotubular array after heat treated at (a) 500 °C (b) 600 °C

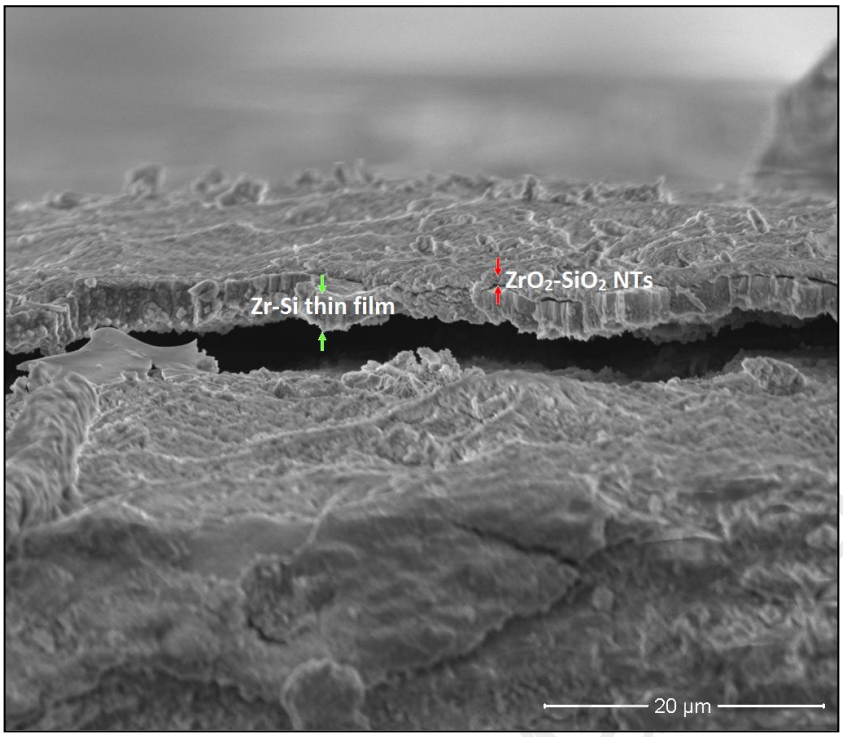

Figure 4.6: Cross sectional FESEM image of Zr-Si thin film and ZrO_2-SiO_2 nanotubular arrays after heat treated at 500 °C.

4.3 EDX Analysis

EDX analysis results showed the elements that present on the surface of modified aluminium alloy series 3, AA3003. Figure 4.7 illustrates that zirconium, silicon and aluminium present after deposition of mixed Zr-Si on Al substrate by PVD method. The analysis shows that the surface covered with 88.02% of Zr, 11.93% of Si and 0.06% of aluminium as shown in Table 4.1. This clearly states that the aluminium substrate has been fully covered with the target materials.

Besides that, Figure 4.8 shows EDX analysis of ZrO_2-SiO_2 nanotubular arrays after anodization. The analysis exhibits that 66.10% of zirconium, 8.48% of silicon, 25.28% of oxygen and 0.13% of aluminium as shown in Table 4.2. The results confirmed the presence of zirconium oxide and silicon oxide as the coating layer by obtaining the oxygen peak with a percentage of 25.28%.

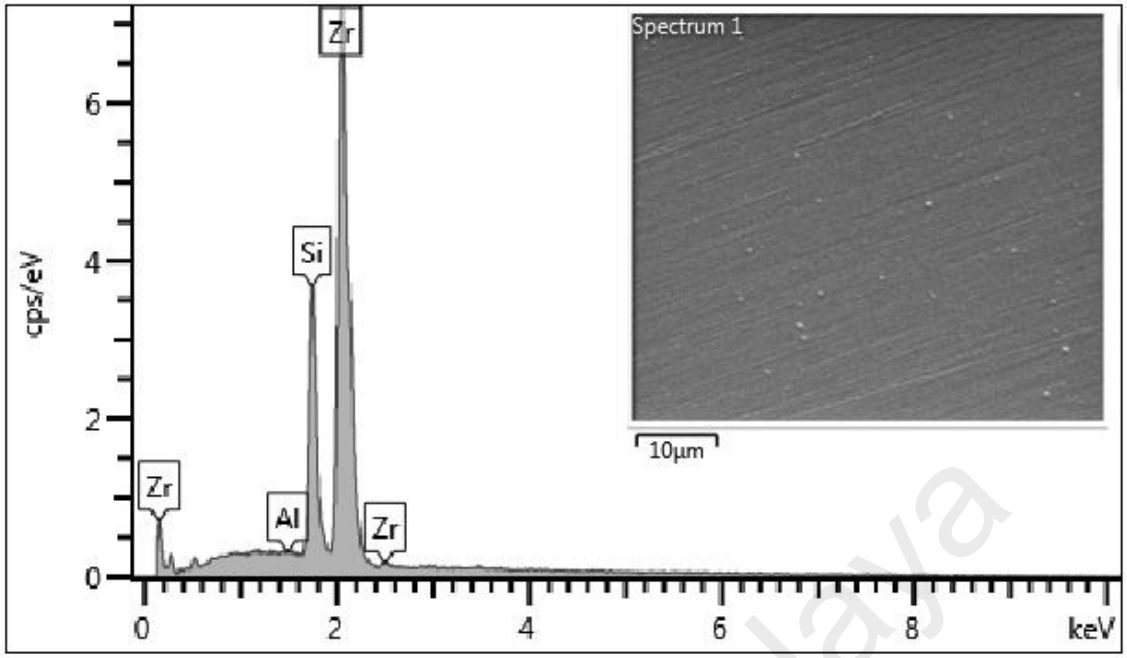

Figure 4.7: EDX analysis of Zr-Si thin film after PVD.

Table 4.1: EDX analysis of Zirconium-Silicon thin film after PVD

Element	Line Type	Wt %	Wt % Sigma	Atomic %
Al	K series	0.06	0.08	0.15
Si	K series	11.93	0.20	30.51
Zr	L series	88.02	0.21	69.34
Total		100.00		100.00

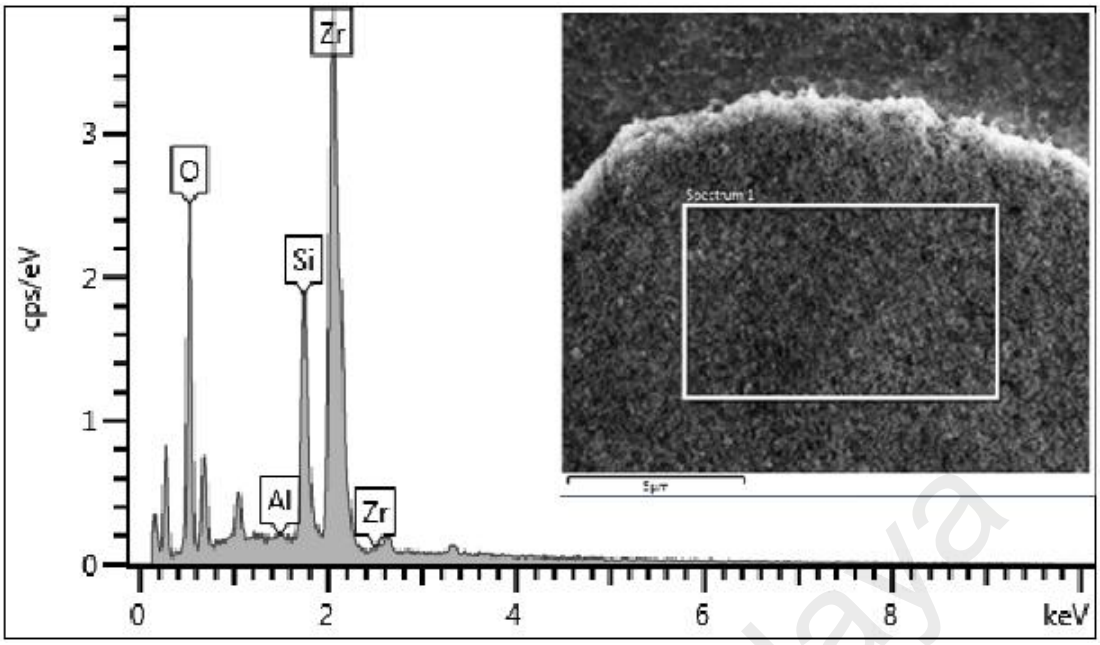

Figure 4.8: analysis of ZrO_2 SiO_2 nanotubular arrays after anodization

Table 4.2: analysis of ZrO_2 SiO_2 nanotubular arrays after anodization

Element	Line Type	Wt %	Wt % Sigma	Atomic %
O	K series	25.28	0.44	60.50
Al	K series	0.13	0.09	0.19
Si	K series	8.48	0.20	11.57
Zr	L series	66.10	0.49	27.74
Total		100.00		100.00

4.4 Mapping Analysis

Mapping analysis shows the distribution of chosen elements on the selected surface. Figure 4.9 shows the distribution of ZrO_2 and SiO_2 nanotubular arrays after anodization process. It can be seen that, the distribution of red colour (Zr) and blue colour (Si) is evenly distributed on the surface and there is no agglomeration of particles in the form of clusters. Thus this feature drives to an excellent wettability and corrosion resistance as an outcome. In a previous study, it has stated that, the thickness of the thin

film layers such that the state of the surfaces can affect on the transport and optical properties. The equal distribution of target material results in smooth bonding surface (Zr-H and Si-H) which improves the wettability of the surface (L.Lawrance, 1988).

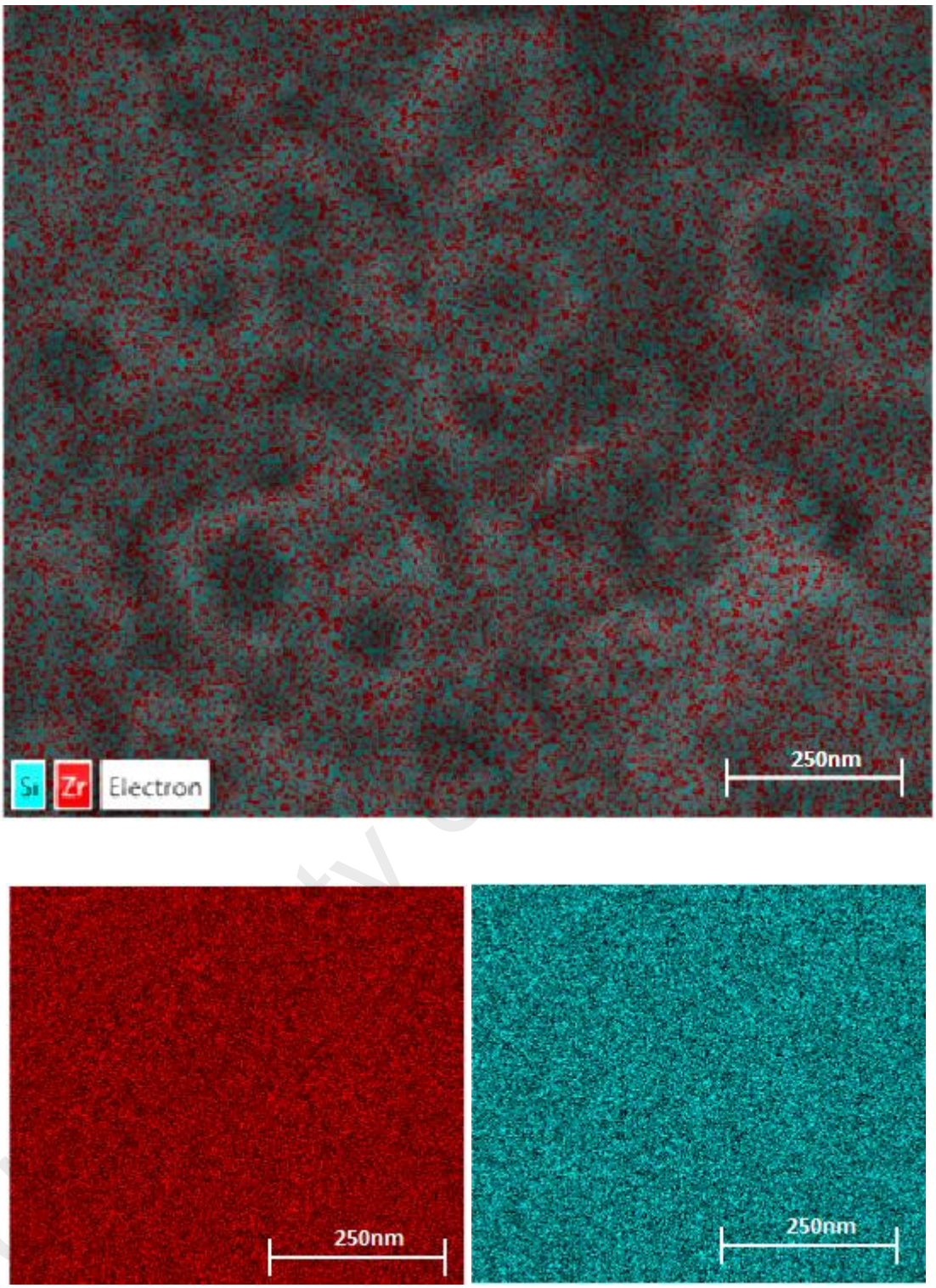

Figure 4.9: The elemental distribution patterns of the constituting elements of the ZrO_2-SiO_2 nanotubular arrays after anodization

4.5 Adhesion strength analysis

The functionality and performance of a thin film is only lie within the mechanical properties but also the adhesion strength between the coated film and substrate that support the film. Figure 4.10 shows the optical micrograph of scratch track and profile of depth, load, friction and coefficient of friction against distance after PVD. Here, the scratch direction was from left to right and the total scratch length was 936.43 μm. The failure point falls at a distance of 543.71 μm as shown in figure 4.10 (a). The load at which the sample failed was 1810 mN.

However figure 4.11 shows the adhesion result of optical micrograph of scratch track and graphs of depth, load, friction, and COF versus distance for the anodized sample after thermal treatment at 600 °C. The total scratch length noted as 985.94 μm and the failure point occurred at a distance of 812.88 μm. The failure load was 2700 mN after heat treated. As expected, the adhesion strength before heat treatment has improved from 1810 mN to 2700 mN after heat treatment. This will eventually result in a better bonding between the substrate and coating.

Hence, heat treatment results in a better adhesion force between substrate and coating which eventually reduce the tendency for the coating to detach from the substrate. The scratch hardness test result shows hardness after deposition of Zr-Si thin film is 12.68GPa while after annealed the hardness has increases to 24.51GPa. Therefore, this concludes that the hardness of sample increased upon subjected to annealing treatment.

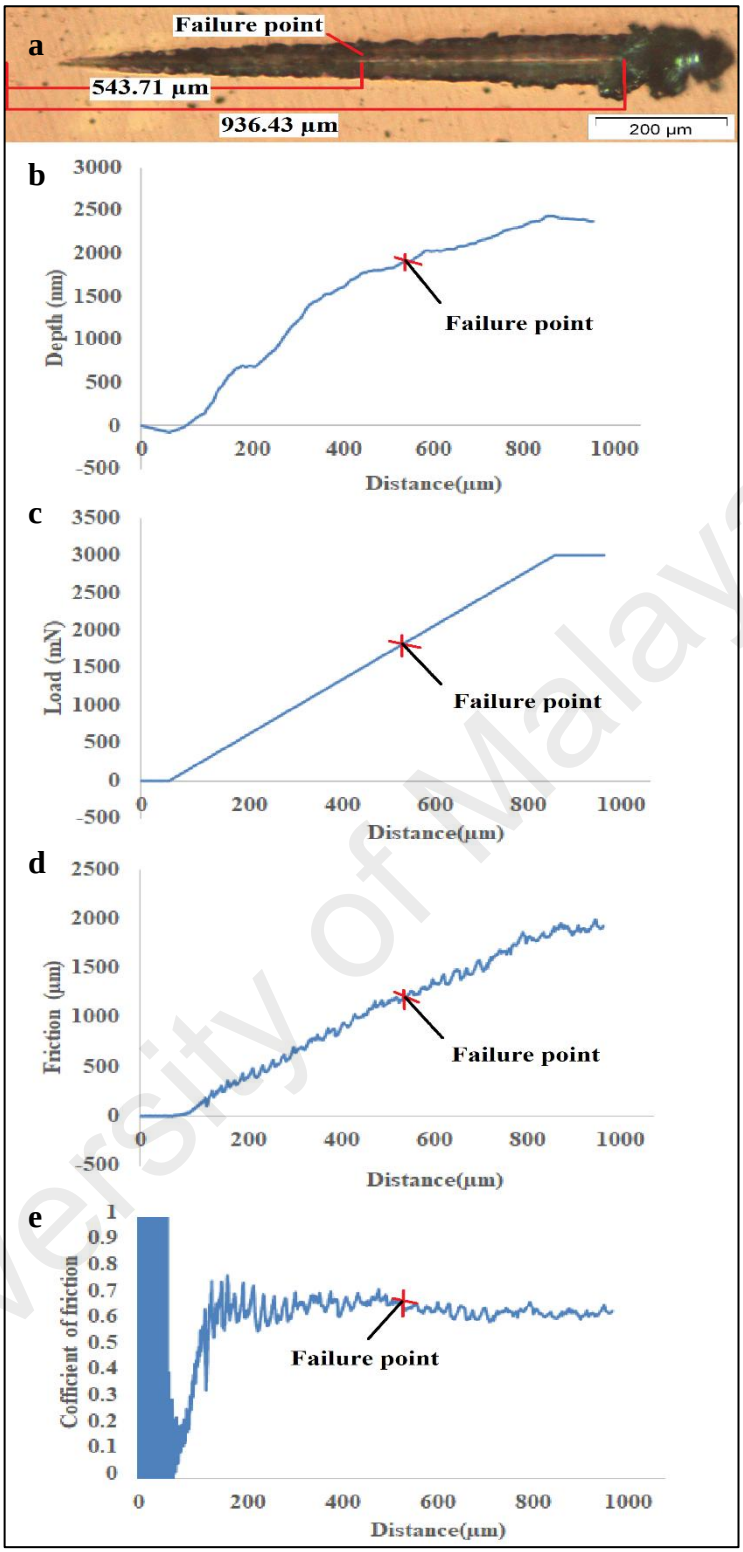

Figure 4.10: (a) The optical micrograph of scratch track and profiles of (b) depth, (c) load, (d) friction and (e) COF against scan distance after PVD.

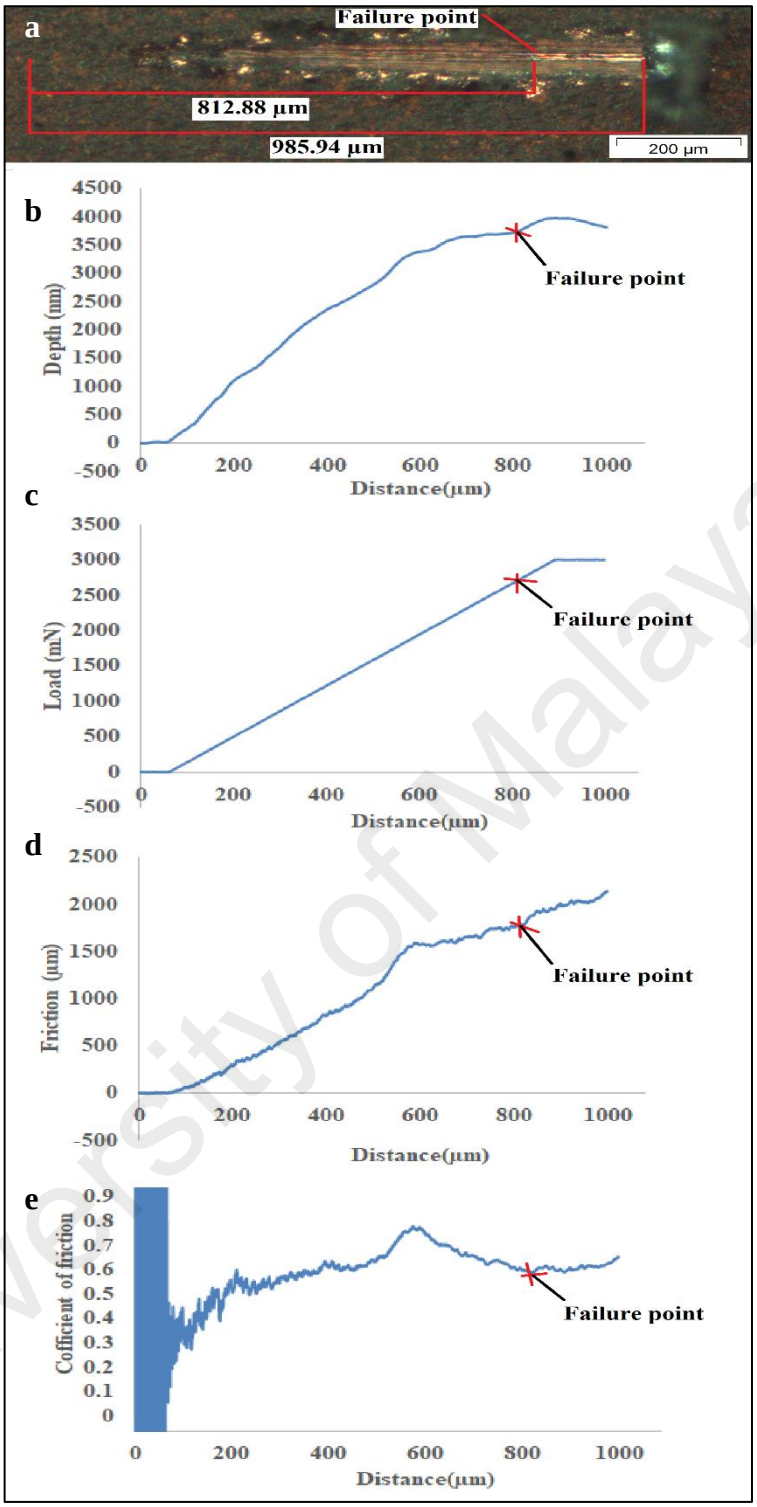

Figure 4.11: Optical micrograph of scratch track and graphs of (b) depth, (c) load, (d) friction, and (e) COF versus distance for the anodized sample after thermal treatment at 600 °C.

4.6 Microhardness Test

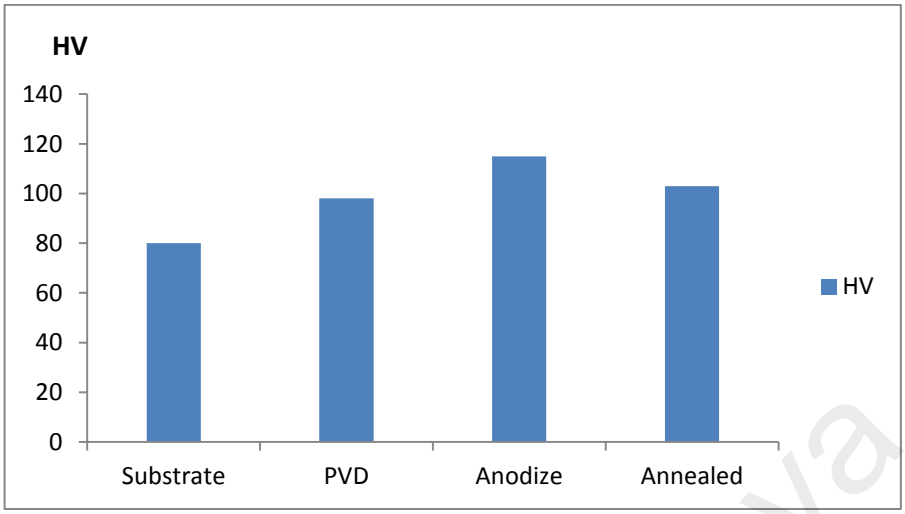

Figure 4.12: Result of microhardness test.

Table 4.3: Microhardness test result.

	Substrate	PVD	Anodize	Annealed
HV	**80**	**98**	**115**	**103**

Figure 4.12 shows the microhardness results for substrate, deposited Zr-Si by PVD, anodized and annealed processes. Substrate shows the lowest hardness value which is 80 HV compared to the PVD process (98 HV). The deposited Zr-Si thin film surface has more endurance towards plastic deformation compared to the substrate itself. Moreover, after anodized and annealed, the hardness values reached 115 and 103 HV, respectively. Thus, the aluminium AA3003 substrate shows better performance and characteristics upon surface modification. Based on previous study, hardness value of aluminium alloy can be increased by means of artificial hardening whereby the solubility if alloying element in aluminium increased markedly with solution treating temperature. However, anodized material has highest hardness value due to during anodization process it produces a hardness coating with large cells and small diameter pores (R.Sadeler, 2006). Similarly, in this present study aluminium alloy AA3003 is

both solution heat treated and artificially aged. Thus the anodized sample has the highest value compare to heat treated and substrate itself.

4.7 Effectiveness of Corrosion Protection

The potentiodynamic polarization method is aimed to characterize the corrosion and passivation kinetics of the samples (Figure 1.13). This study was performed on the substrate (AA 3003), as-deposited PVD, anodized and heat treated samples which were exposed to artificial sea water medium. The results of corrosion potential (*E*corr), corrosion current density (*I*corr) and corrosion rate are summarized in Table 4.4. *E*corr denotes the tendency for the substrate to corrode whilst *I*corr represent the effective of corrosion protection. From Table 4.4, the *E*corr values falls within the range of -670 mV to -790 mV for all the tested samples. The *I*corr value of substrate (AA3003) is 5.432 μA while after deposition of Zr-Si is 4.934 μA. The values then further decreased to 4.870 μA for ZrO_2-SiO_2 nanotubes and finally 3.201 μA for heat treated sample.

Corrosion rate for substrate alone shows 2.328×10^{-6}, while after deposition of Zr-Si thin film, the corrosion rate gradually decreased to 1.752×10^{-6}. This explains that the deposition of thin film on the substrate helps to minimize the corrosion rate by protecting the surface from attack by corrosive environment. Besides that, the corrosion rate for anodized ZrO_2-SiO_2 shows even lower corrosion rate which 1.567×10^{-6} and the value reduces to 1.489×10^{-6} after annealing. Thus, the corrosion rate decreases the substrate undergoes anodization and annealing as well. Furthermore, as expected the corrosion protection efficiency increases from 27.58, 59.31 and 61.32 for after PVD, anodized and annealed samples, respectively. Hence, the surface modification of aluminium alloy series 3 (AA3003) shows a positive outcome towards corrosion

resistance and has the tendency to increase the durability and life span of material during operating.

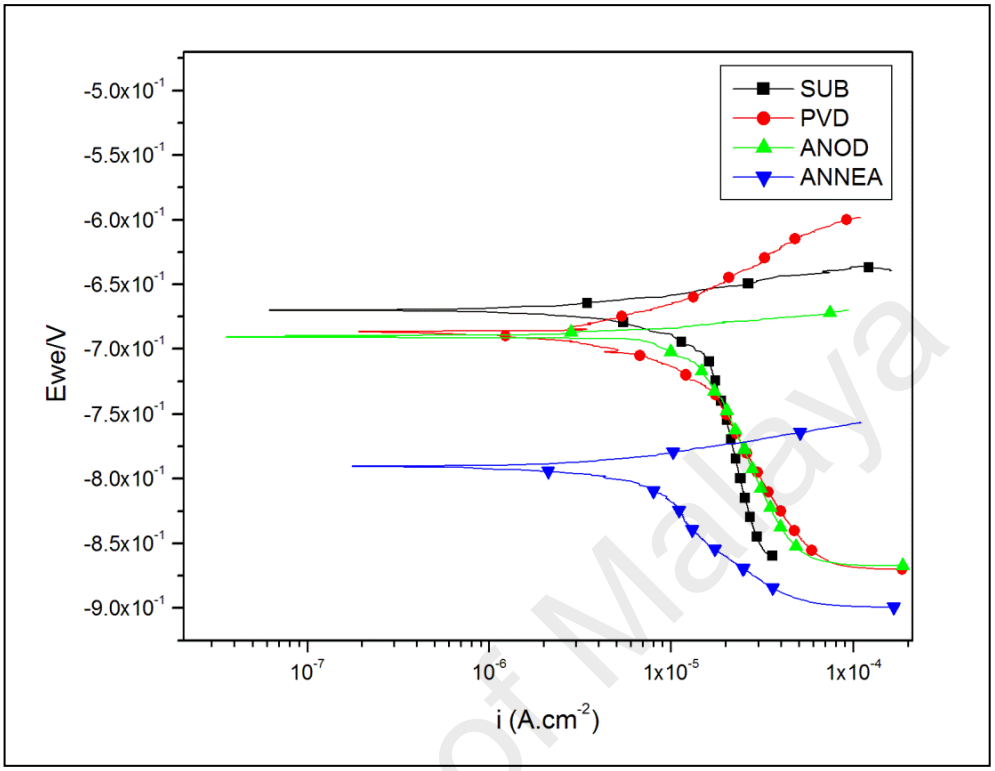

Figure 4.13: Polarization curves of (a) substrate, (b) Zr Si thin film after PVD (c) ZrO_2-SiO_2 nanotubular arrays after anodization, and (d) the heat treated sample at 600 °C for 1.5 h in artificial sea water.

Table 4.4: Corrosion potential (*E*corr), corrosion current density (*I*corr), polarization resistance (*Rp*), corrosion rate and effectiveness of corrosion protection (*P.E.*) values.

Al S3,Zr Si, ZrO_2 SiO_2	Substrate	PVD	Anodized	Annealing
Ecorr / mV	-670.046	-685.779	-689.653	-790.573
Icorr / A	5.432×10^{-6}	3.934×10^{-6}	2.210×10^{-6}	2.101×10^{-6}
log (|<I>/A|)				
Sample weights(gr)	2.4	2.5	2.6	2.6
Density(g/cm3)	2.73	5.26	4.8013	4.8013
E.W(g)	9	18.025	26.1825	26.1825
Corrosion rate	2.328×10^{-6}	1.752×10^{-6}	1.567×10^{-6}	1.489×10^{-6}
P.E	-	27.58	59.31	61.32

4.8 Surface Wettability

Nanoporous films attained by anodization process has different surface wettability (hydrophilicity) depending on the process parameters that been used. Basically, by measuring the surface energy, it is possible to obtain the surface wettability through determination of contact angle ϑ.

As expected, anodization plays a vital role in determining the surface wettability of a material. The contact angle of substrate was ϑ = 90.05° as presented in Figure 4.14 (a). After deposition of thin film of Zr-Si on the surface of material, the contact angle reduced to 52.0°. Upon anodization, the hydrophilicity of the surface improved that is the contact angle further reduced to 24.1° due to the formation of porous structure as shown in Figure 4.15 (c). Figure 4.15 (d) shows the contact angle after heat treatment process. A highly ordered nanotubular arrays formed during annealing at 500 °C due to the transition from an amorphous to a highly crystalline structure resulting in an

improvement of hydrophilicity. The contact angle after heat treatment process showed only 14.0°. Hence it can be concluded that due to the presence of oxide layer and rough surface during anodization, the surface wettability has improved drastically. In a previous literature by E. Zalnezhad *et al*., 2016, it was stated that, anodized sample has better hydrophilicity of the surface due to formation of porous structure while annealed sample has even enhanced hydrophilicity due to highly ordered nanotubular array caused by transition from an amorphous to highly crystalline structure during annealing.

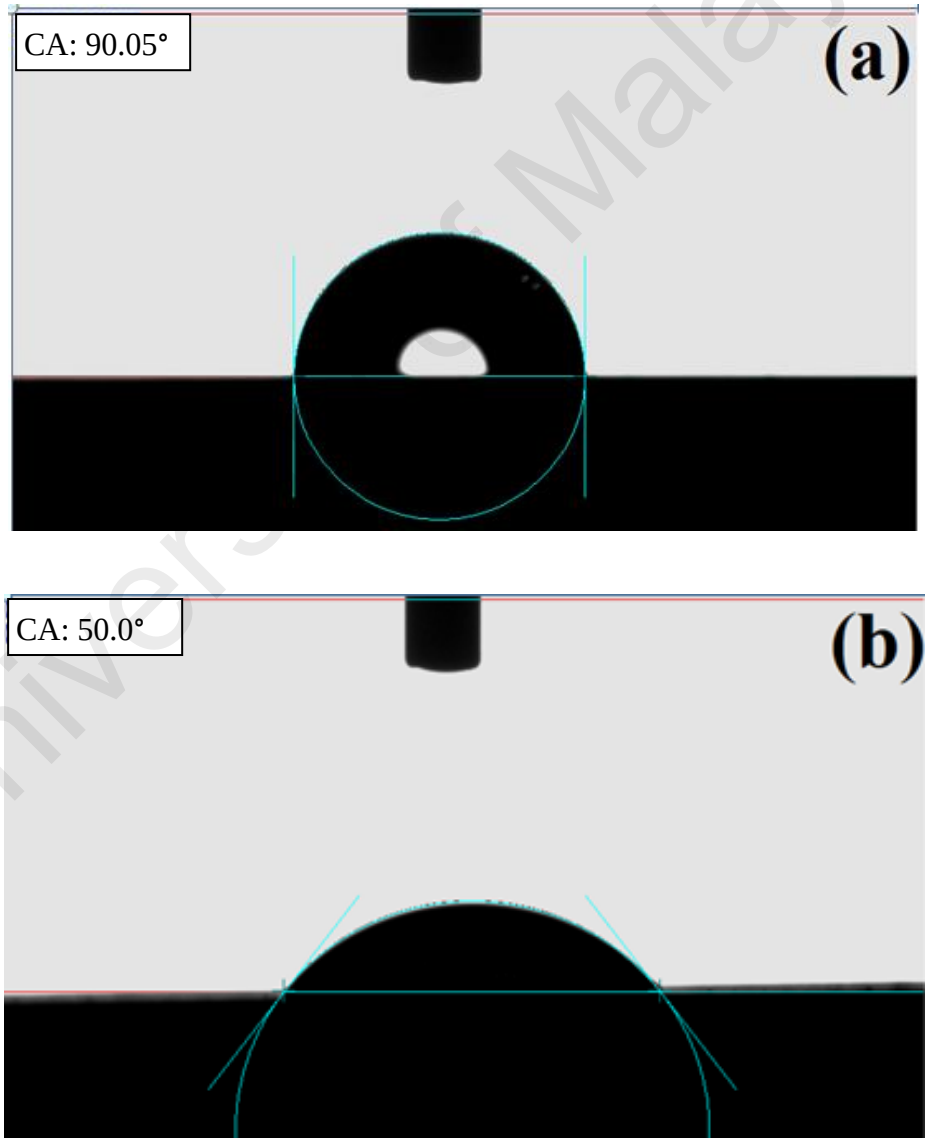

Figure 4.14: Optical images of the contact angles of (a) substrate, (b) Zr Si thin film after PVD

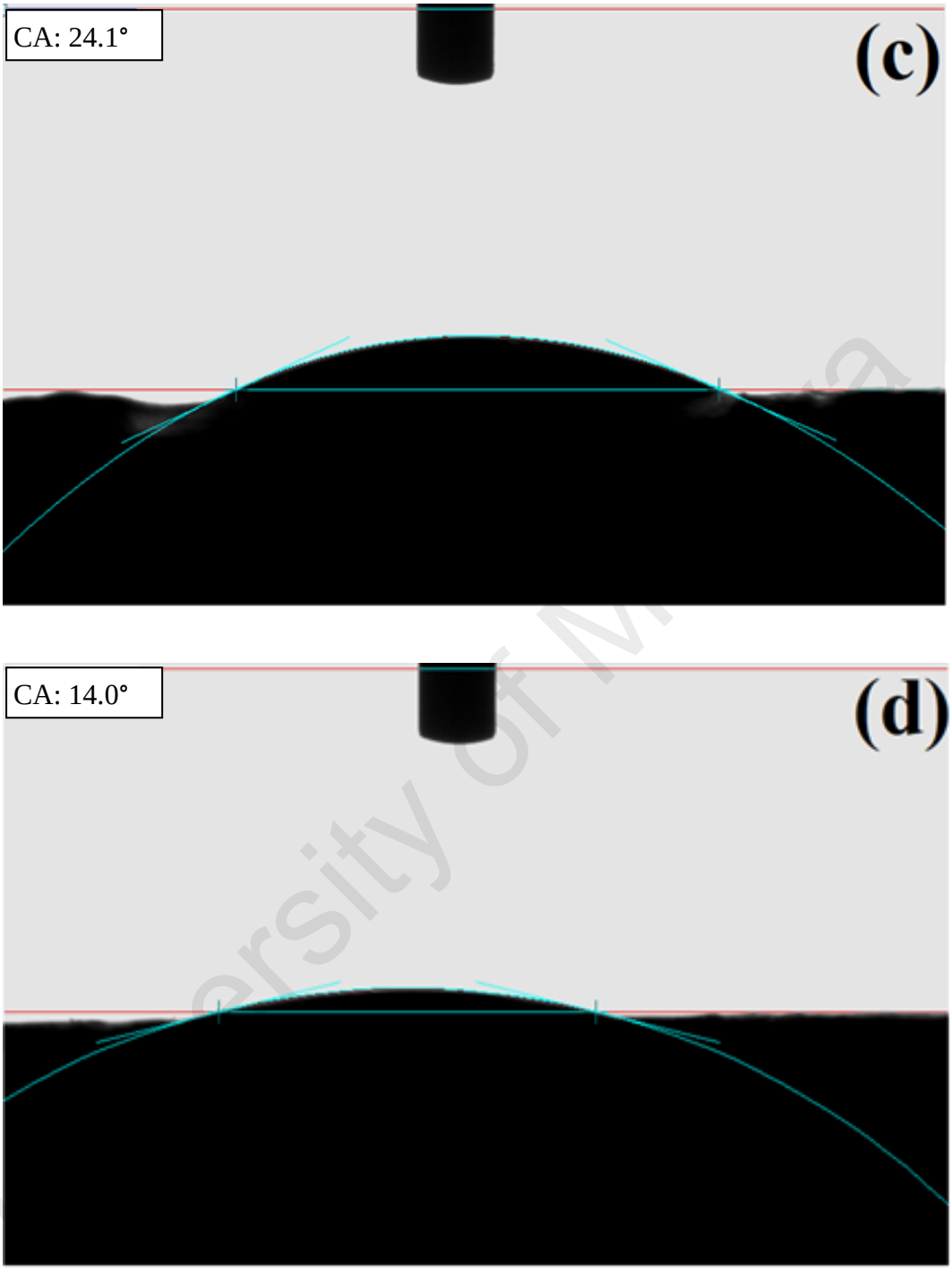

Figure 4.15: (c) ZrO_2-SiO_2 nanotubular arrays after anodization, (d) the heat treated sample at 500 °C for 1.5 h.

CHAPTER 5: CONCLUSION AND RECOMMENDATION

5.1 Conclusion

As a conclusion, in this present study zirconium and silicon targets successfully deposited on the surface of aluminium alloy AA3003 by using PVD method. By using anodizing process with glycerol as an electrolyte, the deposited Zr-Si thin film successfully formed ZrO_2-SiO_2 nanotubular array on the surface of the substrate. Thus, characterization study of corrosion behaviour for the nanotubular array on corrosion behaviour properties carried out for substrate, after deposition of Zr-Si thin film, anodization and heat treatment processes. Surface characterization using FESEM suggest that , after deposition of Zr-Si by PVD, anodization and heat treatment positive impact on the surface morphology of AA3003 compared to substrate itself obtained.

The XRD peaks analysis confirmed that the surface of AA 3003 is covered by Zr and Si elements after PVD process and ZrO_2-SiO_2 peaks after anodization and heat treatment. Thus this proven the presence of ZrO_2-SiO_2 nanotubes as illustrated in FESEM images. Findings from adhesion strength analysis reveals that the heat treated sample has higher failure load compared to the substrate with deposited with Zr-Si. The failure load improves from 1810 mN to 2700 mN. Thus, it suggests that heat treated sample surface can withstand higher load compare to substrate before failure. Moreover, the scratch hardness result also proven that there is a increase in hardness value from 12.68 GPa to 24.51 GPa. The wettability results of heat treated sample which has experience anodization process has lowest contact angle which is 14° compared to substrate AA3003 and Zr-Si thin film coated substrate samples. This analysis suggesting that the surface has a good hydrophilic characteristic which expectedly improves

corrosion rate as well. This put forward that, the modified surface has excellent properties for hydrophilic applications.

This current study, microhardness of the modified surface also determined to analyse the corrosion behaviour. As a result, the anodized and heat treated samples has higher hardness value compared to substrate and after deposition of Zr-Si thin film sample. The higher hardness value signifying that the modified surface has better corrosion protection. The polarization curve confirmed that the corrosion rate decreases gradually from substrate to after deposition of Zr-Si thin film which is 2.328×10^{-6} to 1.752×10^{-6}. Upon completion of anodization and heat treatment it enhances corrosion protection even more by resulting in lower corrosion rate. The corrosion rate of anodized sample is 1.567×10^{-6} and after heat treatment the rate further decreases to 1.489×10^{-6}. Hence, the modified nanoporous surface shows better corrosion behaviour.

Current research work is aimed to fabricate and develop ZrO_2-SiO_2 NTs array by PVD and study the corrosion behaviour of AA 3003. The results of the testing showed the nanotubular array oxide layer gives additional strength, good wettability, lower corrosion rate and excellent microhardness value. The novelty of this study is to fabricate Zr-Si thin film on AA 3003 substrate and develop ZrO_2-SiO_2 nanotubular array to improves corrosion resistance of AA 3003. The results that obtained can be used as reference for further studies.

5.2 Recommendation

As a recommendation, more studies need to conduct in order to have a greater view in wider aspects. Tribo-corrosion characteristics are one of the

fields that needed to venture and study thoroughly as corrosion and wear is one of a major drawback in any metals.

Besides that, the modified surface can be studied in terms of biocompatibility whereby the material characterization can be carried in biodiesel or palm oil to widen the application in many other industries such as automotive. Jurgen et al., 2014 mentioned in the report that due to the rising economic and political pressure to reduce fuel consumption and CO_2 emission, effort made to use light weight material such as aluminium even more in automotive applications with the aid of surface modification to increase the lifespan of the components. Apart from that, Super-Light-Car (SLC) concept shows application of aluminium for the car body can be an advantage of at least 30% without degrading any of its performance (Hirsch,J *et al.,* 2002).

REFERENCES

Andritschky, M. (1995). Protective coatings on high temperature steel applied by PVD deposition techniques. *Journal of materials processing technology*, *53*(1-2), 33-46.

Ardakani, S. R., Afshar, A., Sadreddini, S., & Ghanbari, A. A. (2017). Characterization of Ni-P-SiO2-Al2O3 nano-composite coatings on aluminum substrate. *Materials Chemistry and Physics*, *189*, 207-214.

A.S.H.Makhlouf. (2011). Current and advanced coating technologies for industrial applications. In I. T. Abdel Salam Hamdy Makhlouf, *Metals and Surface Engineering* (pp. 3-23). Woodhead.

Association, A. (1984). Aluminium: Properties and physical metallurgy. In J. Hatch (Ed). ASM International, Materials Park Ohio.

Ahmad, Z. (2006). ANODIZED COATINGS. *Principles of Corrosion Engineering and Corrosion Control* , 382-437.

Alpagut Kara, M. J. (2004). An application for zirconia as a pharmaceutical die set. *Journal of the European Ceramic Society* , 3091-3101.

Andritschky, M. (1995). Protective coatings on high temperature steel applied by PVD deposition techniques. *Meterial Processing Technology 53* , 33-46.

Antonio Facchetti, E. A. (2004). Very large electro-optic responses in H-bonded heteroaromatic fi lms grown by physical vapour deposition. *Nature Materials 3* , 910-917.

Avner, S. H. (1964). I*ntroduction to Physical Metallurgy*. New York: McGraw-Hill.

Bewilogua, K., Bräuer, G., Dietz, A., Gäbler, J., Goch, G., Karpuschewski, B., & Szyszka, B. (2009). Surface technology for automotive engineering. *CIRP Annals-Manufacturing Technology*, *58*(2), 608-627.

Braceras, I., Ibáñez, I., Taher, M., Mao, F., del Barrio, A., De Urturi, S. S., ... & Jansson, U. (2018). On the electro-tribological properties and degradation resistance of silver-aluminum coatings. *Wear*, *414*, 202-211.

B.Raj, K. S. (2016). Mechanical Testing Overview. In *Materials Science and Materials Engineering* (pp. 5277-5290). Elsevier.

Cerezo, J., Vandendael, I., Posner, R., De Wit, J. H. W., Mol, J. M. C., & Terryn, H. (2016). The effect of surface pre-conditioning treatments on the local composition of Zr-based conversion coatings formed on aluminium alloys. *Applied Surface Science*, *366*, 339-347.

Carle, D., & Blount, G. (1999). The suitability of aluminium as an alternative material for car bodies. *Materials & design*, *20*(5), 267-272.

Carlsson, P., & Olsson, M. (2006). PVD coatings for sheet metal forming processes—a tribological evaluation. *Surface and Coatings Technology*, *200*(14-15), 4654-4663.

Cole, GS, S.A. (1995). Lightweight materials for automotive applications. Material Characteristics, 3-9.

Davis, J.R. (1993). ASM speciality handbook: aluminium and aluminium alloy. ASM International, Materials Park Ohio.

Demir, H., & Gündüz, S. (2009). The effects of aging on machinability of 6061 aluminium alloy. *Materials & Design*, *30*(5), 1480-1483.

Díaz-Ballote, L., López-Sansores, J. F., Maldonado-López, L., & Garfias-Mesias, L. F. (2009). Corrosion behavior of aluminum exposed to a biodiesel. *Electrochemistry Communications*, *11*(1), 41-44.

D.Regonini, A. R. (2010,42). Effect of heat treatment on the properties and structure of TiO2 nanotubes: phase composition and chemical composition. *Surface interface analysis* , 139-144.

Dunstan Barnes, S. J. (2012). Using scratch testing to measure the adhesion strength of calcium phosphate coatings applied to poly(carbonate urethane) substrates. *Mechanical behaviour of biomedical materials 6* , 128-138.

Gaurav Verma, M. D. (2017). *Nano- and Microscale Drug Delivery Systems.* Elsevier.

Gerrard Eddy Jai Poinern, N. A. (2011). Progress in Nano-Engineered Anodic Aluminum Oxide Membrane Development. *Materials* , 487-526.

Gudla, V. C., Canulescu, S., Shabadi, R., Rechendorff, K., Dirscherl, K., & Ambat, R. (2014). Structure of anodized Al–Zr sputter deposited coatings and effect on optical appearance. *Applied Surface Science*, *317*, 1113-1124.

Esfe, M. H., Yan, W. M., Afrand, M., Sarraf, M., Toghraie, D., & Dahari, M. (2016). Estimation of thermal conductivity of Al2O3/water (40%)–ethylene glycol (60%) by artificial neural network and correlation using experimental data. *International Communications in Heat and Mass Transfer*, *74*, 125-128.

E. Hollingsworth, H.H. (1987). Metals handbook. ASM International.

Golru, S. S., Attar, M. M., & Ramezanzadeh, B. (2015). Morphological analysis and corrosion performance of zirconium based conversion coating on the aluminum alloy 1050. *Journal of Industrial and Engineering Chemistry*, *24*, 233-244.

Gudla, V. C., & Ambat, R. (2015). Optically Designed Anodised Aluminium Surfaces: Microstructural and Electrochemical Aspects. Kgs. Lyngby: Technical University of Denmark (DTU).

Gustafsson, S. (2011). *COrrosion properties of aluminium alloys and surface treated alloys in tap water.* Annika Pohl: Uppsala Universitet.

Hatch, J. (1984). Aluminium properties and physical metallurgy. Metals Park (OH): ASM.

Habazaki, H., Fushimi, K., Shimizu, K., Skeldon, P., & Thompson, G. E. (2007). Fast migration of fluoride ions in growing anodic titanium oxide. *Electrochemistry communications*, *9*(5), 1222-1227.

Hirsch, J. (2014). Recent development in aluminium for automotive applications. *Transactions of Nonferrous Metals Society of China*, *24*(7), 1995-2002.

Huanca, D. R., Kim, H. Y., & Salcedo, W. J. (2015). Silicon microtubes made by immersing macroporous silicon into ammonium fluoride solution. *Materials Chemistry and Physics*, *160*, 12-19.

Hwaiyu Geng, C. P. (2005). *Semiconductor Manufacturing Handbook.* New York: McGraw-Hill Education.

Hoeppner, D. (1985). Pitting Corrosion: morphology and characterization.

Hovsepian, P. E., Luo, Q., Robinson, G., Pittman, M., Howarth, M., Doerwald, D., ... & Zeus, T. (2006). TiAlN/VN superlattice structured PVD coatings: a new alternative in machining of aluminium alloys for aerospace and automotive components. *Surface and coatings technology*, *201*(1-2), 265-272.

In L. W.McKeen, (2006). *Fluorinated Coatings and Finishes Handbook* (pp. 99-107). William Andrew.

I.J., P. (2015). Wrought aluminium alloys in Light alloys (4th ed.). Oxford:Butterworth-Heinemann.

Internatrional, A. (1987). Metals Handbook, Ninth Edition: Volume 13-Corrosion (ASM Handbook). ASM International Ohio.

Isobe, T., Tomita, T., Kameshima, Y., Nakajima, A., & Okada, K. (2006). Preparation and properties of porous alumina ceramics with oriented cylindrical pores produced by an extrusion method. *Journal of the European Ceramic Society*, *26*(6), 957-960.

J. Banerjee, E. H. (2018). *Self-assembling peptides and their application in tissue engineering and regenerative medicine.* Woodhead Publishing.

Jehn, H. A. (2000). Improvement of the corrosion resistance of PVD hard coating–substrate systems. *Surface and Coatings Technology*, *125*(1-3), 212-217.

J.A. Wharton, R.B. (2005). Corrosion Science. 47, 3336-3367.

J.R. Davis. (1999). Corrosion of aluminium and Aluminium Alloys. USA: ASM International.

Kaufman, J. (2000). Introduction to aluminium Alloys and Tempers. ASM International.

K.Reichelt, X. (1990). The preparation of thin film by physical vapour deposition methods. *Thin Solid Films, 191* , 91-126.

Ke, Z. U. O., Xin, W. A. N. G., Wei, L. I. U., & Yue, Z. H. A. O. (2014). Preparation and characterization of Ce-silane-ZrO2 composite coatings on 1060 aluminum. *Transactions of Nonferrous Metals Society of China*, *24*(5), 1474-1480.

Kim, J. H., Jeong, G. Y., Kim, S., Jeong, Y. J., & Sohn, D. S. (2018). Effect of coating thickness and annealing temperature on ZrN coating failure of U-Mo particles under heat treatment. *Journal of Nuclear Materials*, *507*, 347-359.

Kiyoshi Okadaz, K. J. (2006). Nanoporous Materials from Mineral and Organic Templates. *Nanomaterials* , 349-382.

Kolla Meheresh Gupta, K. R. (2018). Cutting Characteristics of PVD Coated Cutting Tools . *Materials Today: Proceedings 5* , 11260-11267.

Koyama, S., Aoki, Y., Nagata, S., Kimura, H., & Habazaki, H. (2010). Amorphous-to-crystalline transition of silicon-incorporated anodic ZrO2 and improved dielectric properties. *Electrochimica Acta*, *55*(9), 3144-3151.

Lawrance, L. (1988). Analysis and charcterization of thin films: A Tutorial. *Solar Cell, 24* , 387-418.

Lee, K., Kim, D., & Yoon, Y. S. (2018). SiC/Si thin film deposited on zircaloy to improved accident tolerant fuel cladding. *Thin Solid Films*.

Leeuw, B. M. (1999). *Corrosion of Aluminium Alloys used in.* Pietermaritzburg: Universiyt of Natal.

Losic, D., & Santos, A. (2015). Nanoporous Alumina. *Nanoporous Alumina: Fabrication, Structure, Properties and Applications, Springer Series in Materials Science, Volume 219. ISBN 978-3-319-20333-1. Springer International Publishing Switzerland, 2015*.

Lunder, O., Simensen, C., Yu, Y., & Nisancioglu, K. (2004). Formation and characterisation of Ti–Zr based conversion layers on AA6060 aluminium. *Surface and Coatings Technology*, *184*(2-3), 278-290.

Luciano, G., Brinkmann, A., Mahanty, S., & Echeverría, M. (2017). Development and evaluation of an eco-friendly hybrid epoxy-silicon coating for the corrosion protection of aluminium alloys. *Progress in Organic Coatings*, *110*, 78-85.

M.G. Debije, A. S. (2016). *Stimuli-Responsive Liquid Crystalline Materials.* Elsevier.

M.G.S.Ferreira, M. J. (2012). Self-healing nanocoatings for corrosion control. *Corrosion Protection and Control using Nanomaterials* , 213-263.

Merlo, A. M. (2003). The contribution of surface engineering to the product performance in the automotive industry. *Surface and Coatings Technology*, *174*, 21-26.

Manoj, K. C., Dubey, M., Bills, B., Al-Qaradawi, I. Y., Lamsal, B. S., Galipeau, D., & Fan, Q. H. (2013, May). Aqueous electrolyte system for porous silicon using electrochemical anodization. In *Electro/Information Technology (EIT), 2013 IEEE International Conference on* (pp. 1-4). IEEE.

Materazzi, S. (2008). *Handbook of Thermal Analysis and Calorimetry.* 439-502.

N. Alsenmo, J.M. (2006). Material Science Engineering A 428.

N.L. Sukiman, X. Z. (2012). Aluminium Alloys- New Trends in Fabrication and Applications. *Intech*, 47-97.

Nurilhuda Bashirom, K. A. (2017). ynthesis of freestanding amorphous ZrO2 nanotubes by anodization and their application in photoreduction of Cr(VI) under visible light. *Surface and Coating Technology* , 317-376.

Oshida, Y. (2013). Bioscience and Bioengineering of Titanium Materials. Elsevier.

0. Knotek, F. L. (1993). Process and advantage of multicomponent and multilayer PVD coatings . *Surface and Coatings Technology*, *59* , 14-20.

Park, M. H., Kim, M. G., Joo, J., Kim, K., Kim, J., Ahn, S., ... & Cho, J. (2009). Silicon nanotube battery anodes. *Nano letters*, *9*(11), 3844-3847.

Pathak, S. S., Sharma, A., & Khanna, A. S. (2009). Value addition to waterborne polyurethane resin by silicone modification for developing high performance coating on aluminum alloy. *Progress in Organic Coatings*, *65*(2), 206-216.

P.bhattacharya, G. L. (2014). Experimental qualification of bone mechanics. In *Bone substitute biomaterials* (pp. 30-71). Woodhead Publishing.

P.Sahoo, S. J. (2017). Surface Finish Coeating. *Comprehensive Material Finishing* , 38-55.

Parkhutik, V., Matveeva, E., Perez, R., Alamo, J., & Beltrán, D. (2000). Mechanism of large oscillations of anodic potential during anodization of silicon in H3PO4/HF solutions. *Materials Science and Engineering: B, 69,* 553-558.

Pragasam Viswanathan, Y. M. (2017). Challenges in oral drug delivery: a nano-based strategy to overcome. *Nanostrauctures for Oral Medicine* , 173-201.

Roberge, P. (2008). Corrosion Engineering. Mc Graw-Hill Education.

Reichelt, K., & Jiang, X. (1990). The preparation of thin films by physical vapour deposition methods. *Thin Solid Films*, *191*(1), 91-126.

R.E.Smallman, A. (2014). Characterization and Analysis. In *Modern Physical Metallurgy* (pp. 159-250). Butterworth Heinemann.

R.Sadeler. (2006). Effect of a commercial hard anodizing on the fatigue property of a 2014-T6 aluminium alloy. *Journals of material science* , 5803.

Sadreddini, S., & Afshar, A. (2014). Corrosion resistance enhancement of Ni-P-nano SiO2 composite coatings on aluminum. *Applied Surface Science*, *303*, 125-130.

Sarraf, M., Zalnezhad, E., Bushroa, A. R., Hamouda, A. M. S., Rafieerad, A. R., & Nasiri-Tabrizi, B. (2015). Effect of microstructural evolution on wettability and tribological behavior of TiO2 nanotubular arrays coated on Ti–6Al–4V. *Ceramics International*, *41*(6), 7952-7962.

Sarraf, M., Razak, B. A., Crum, R., Gamez, C., Ramirez, B., Kasim, N. H. B. A., ... & Basirun, W. J. (2017). Adhesion measurement of highly-ordered TiO2 nanotubes on Ti-6Al-4V alloy. *Processing and Application of Ceramics*, *11*(4), 311-321.

Schweitzer,P. (2003). *Metallic material: Physical, mechanical and corrosion*. New York: CRC Press.

Sun, Y. M., Lozano, J., Ho, H., Park, H. J., Veldman, S., & White, J. M. (2000). Interfacial silicon oxide formation during synthesis of ZrO2 on Si (100). *Applied surface science*, *161*(1-2), 115-122.

Scully, J. (1990). *The Fundamentals of corrosion* (3 ed). Oxford: Pergamon.

SH, A. (1974). Introduction to physical metallurgy (2 ed). New York: McGraw-Hill.

Sweetu B. Patel, N. B. (2017). Transparent TiO2 nanotubes on zirconia for biomedical applications. *RSC Advances* , 30397.

Said Jahanmir, X. Dong, Wear mechanisms of aluminum oxide ceramics, Friction and wear of ceramics, 15-50 (1994).

Tsao, Y. C., Fisker, C., & Pedersen, T. G. (2014). Optical absorption of amorphous silicon on anodized aluminum substrates for solar cell applications. *Optics Communications*, *315*, 17-25.

Thirupathi, K., Bárczy, P., Vad, K., Csik, A., & Somosvári, B. M. (2018). Effects of vacuum and ageing on Zr4/Cr3 based conversion coatings on aluminium alloys. *Applied Surface Science*, *441*, 1043-1047.

Tribology of ceramics, Report of the Committee on Tribology of Ceramics, National Academies, 1988, 110.

Tucci, A., & Esposito, L. (1994). *Microstructure and tribological properties of ZrO2* ceramics. *Wear*, *172*(2), 111-119

Thomas Bjork, R. W. (1999). P*hysical vapour deposition duplex coatings for aluminium extrusion dies*. *Wear 225-229* , 1123-1130.

Toshihiro Tanaka, J. L. (2014). Interfacial free energy and wettability. In *Treatise on Process Metallurgy* (pp. 61-77). Sweden: Royal Institute of Technology .

Vargel, C. (2004). Corrosion of Aluminium. Paris: Elsevier

Vencl, A., Rac, A., & Bobic, I. (2004). Tribological behaviour of Al-based MMCs and their application in automotive industry. *Tribology in industry*, *26*(3-4), 31-38.

Verardi, P., Craciun, F., Mirenghi, L., Dinescu, M., & Sandu, V. (1999). An XPS and XRD study of physical and chemical homogeneity of Pb (Zr, Ti) O3 thin films obtained by pulsed laser deposition. *Applied surface science*, *138*, 552-556.

WC, W. (1992). A brief introduction to advanced surface modification technologies. *J Oral Implantol* , 18(3):231-5.

Yu, M., Xue, B., Liu, J., Li, S., & Zhang, Y. (2015). Electrophoretic deposition of hybrid coatings on aluminum alloy by combining 3-aminopropyltrimethoxysilan to silicon–zirconium sol solutions for corrosion protection. *Thin Solid Films*, *590*, 33-39.

Zant, P. V. (2014). *Microchip Fabrication.* New York: McGraw-Hill Education.

Zalnezhad, E. (2016). Effect of structural evolution on mechanical properties of ZrO2 coated Ti–6Al–7Nb-biomedical application. *Applied Surface Science*, *370*, 32-39.

Zuo, X., Li, W., Mu, S., Du, J., Yang, Y., & Tang, P. (2015). Investigation of composition and structure for a novel Ti–Zr chemical conversion coating on 6063 aluminum alloy. *Progress in Organic Coatings*, *87*, 61-68.